

# Bulk electric conductivity response to soil and rock CO<sub>2</sub> concentration during controlled CO<sub>2</sub> release experiments: Observations and analytic modeling

Scott Jewell<sup>1</sup>, Xiaobing Zhou<sup>1</sup>, Martha E. Apple<sup>2</sup>, Laura M. Dobeck<sup>3</sup>, Lee H. Spangler<sup>3</sup>, and Alfred B. Cunningham<sup>4</sup>

## ABSTRACT

To develop monitoring technologies for geologic CO<sub>2</sub> storage, controlled CO<sub>2</sub> release experiments at the Zero Emissions Research and Technology (ZERT) site in Bozeman, Montana, USA, were carried out in 2009–2011. To understand the impact on the electric properties of soil and sediment rock due to possible CO<sub>2</sub> leakage, we have developed an analytical model to explain and predict the electric conductivity (EC) for CO<sub>2</sub> impacted soil and sedimentary rock. Results from the model were compared with the measurements at the ZERT site during 2009–2011 and the CO<sub>2</sub>-Vadose Project site in France in 2011–2012 after model calibration at each site. The model was calibrated

using the saturation ( $n$ ) and cementation ( $m$ ) exponents contained in Archie's equation, and a chemistry coefficient ( $pKc$ ) as tuning parameters that minimized the misfit between observed and modeled soil/rock bulk conductivity data. The calibration resulted in  $n = 3.15$ ,  $m = 2.95$ , and  $pKc = 4.7$  for the ZERT site, which was within the range of values in the literature. All the ZERT data sets had rms errors of 0.0115–0.0724. For the CO<sub>2</sub>-Vadose site, calibration resulted in  $n = 3.6$ – $9.85$  and  $m = 2.5$ – $4.2$ ,  $pKc = 4.80$ – $5.65$ , and the rms error of 0.0002–0.0003; the cementation exponents were consistent with the literature. These results found that the model predicted the bulk EC reasonably well in soil and rock once the unmeasurable model parameters ( $n$ ,  $m$ , and  $pKc$ ) were calibrated.

## INTRODUCTION

With the increasing concentration of atmospheric CO<sub>2</sub>, there has been some concern on the effects of this greenhouse gas on climate change. This concern has led to research on technologies of mitigating the increasing concentration of atmospheric carbon either by counteracting the effects or by removing the gas from the atmosphere. One method that is receiving extensive attention is geologic carbon sequestration, where CO<sub>2</sub> is injected into geologic formations for long-term storage (Holloway, 2001). Pilot projects are underway all over the world including Sleipner in the North Sea, the Otway Basin Pilot Project in Australia (Shukla et al., 2010), the CO<sub>2</sub> SINK in Germany (Kiessling et al., 2010), and SECARB in the United States (Hovorka et al., 2011). There are a variety of geo-

logic formations that can be used for geologic sequestration: depleted oil and gas fields, deep saline aquifers, and unminable coal seams (Holloway, 2001; Zhou et al., 2013). In active oil and gas fields and in coal bed methane production, CO<sub>2</sub> has already been used for enhanced oil production (Shukla et al., 2010). In saline aquifers, CO<sub>2</sub> will dissolve in the water and react with other chemicals dissolved therein to form carbonate minerals (Xiao et al., 2009). This mineral sequestration process takes thousands of years to complete, and so a reservoir should have a minimum of leakage over that time frame.

Although geologic sequestration can provide a method of reducing atmospheric carbon, care must be taken to monitor the CO<sub>2</sub> to ensure it is not leaked back into the atmosphere. The probability of leakage depends on the permeability and frequency of fractures in the strata overlying the reservoir; the primary leakage vectors are

Manuscript received by the Editor 8 March 2014; revised manuscript received 26 March 2015; published online 1 September 2015.

<sup>1</sup>Montana Tech of The University of Montana, Department of Geophysical Engineering, Butte, Montana, USA. E-mail: shjewell@mtech.edu; xzhou@mtech.edu.

<sup>2</sup>Montana Tech of The University of Montana, Department of Biological Sciences, Butte, Montana, USA. E-mail: mapple@mtech.edu.

<sup>3</sup>Montana State University, Energy Research Institute, Bozeman, Montana, USA. E-mail: dobeck@chemistry.montana.edu; spangler@montana.edu.

<sup>4</sup>Montana State University, Department of Civil Engineering, Bozeman, Montana, USA. E-mail: al\_c@erc.montana.edu.

© 2015 Society of Exploration Geophysicists. All rights reserved.

faults and fractures in the caprock of the reservoir (Zhang et al., 2009) or through permeating via migration (Li et al., 2006; Liu et al., 2012). To this end, many geophysical techniques can be used to monitor CO<sub>2</sub> and its migration underground (Kiessling et al., 2010; Hovorka et al., 2011), with varying outcomes (Gasperkova and Hoversten, 2006; Arts et al., 2009). Electric conductivity (EC) measurements or electric resistivity tomography (ERT) has been shown to be an effective method for monitoring CO<sub>2</sub> in boreholes (Al Hagrey, 2011; Breen et al., 2012; Carrigan et al., 2013). CO<sub>2</sub> is often injected into reservoirs in its supercritical phase. Cross-hole and surface-downhole ERT measurements can be used to monitor the electric resistivity change in a reservoir due to the injected supercritical CO<sub>2</sub> plume (Kiessling et al., 2010; Fabriol et al., 2011). Supercritical CO<sub>2</sub> can flow through rocks but has different material properties from gaseous or aqueous CO<sub>2</sub> dissolved in water (Al Hagrey, 2011). Much of the literature on EC monitoring at the reservoir level deals with supercritical CO<sub>2</sub>. However, literature on monitoring and diagnosing CO<sub>2</sub> leakage into the near surface including shallower aquifers using resistivity method has been published recently (Strazisar et al., 2009; Zhou et al., 2012; Dafflon et al., 2013). In the following discussion, the different phases of carbon dioxide or CO<sub>2</sub> will be referred to as gas CO<sub>2</sub>, aqueous CO<sub>2</sub> when dissolved in water, or supercritical CO<sub>2</sub> (liquid), etc.

Monitoring the EC of the soils or porous rocks in the vadose zone above an injection site for leak detection can be done simply and inexpensively. Modern probes containing multiple instruments are inexpensive and accurate, and data collection can be automated (Bristow et al., 2001; Zhou et al., 2012). Recent work at the Zero Emissions Research and Technology (ZERT) site in Bozeman, Montana, USA, has shown that CO<sub>2</sub> gas has a tendency to move in a preferential path through soils, causing small areas of the surface with high concentration of soil CO<sub>2</sub> and visible earlier senescence or dieback of vegetation (grass and dandelion) (Spangler et al., 2009; Lakkaraju et al., 2010; Sharman et al., 2014). These areas are called hot spots. The development of a technique that can determine and delineate these hot spots remotely would improve the safety and reduce the cost of monitoring sequestration projects.

There are many factors that determine bulk soil EC or electric resistivity (ER) (Banisi et al., 1993), some of which are unique to the soil or rock's physical properties, such as clay content and natural salinity that are stable over time in a particular location. As long as the soil is undisturbed, the soil's geometric contribution, that of the orientation and shape of the soil particles, can be held as a constant (Seger et al., 2009). Factors that can change over short periods of time are the volumetric water content (VWC) (or soil moisture) (Rhoades and Corwin, 1990; Banisi et al., 1993; Friedman, 2005; Samouëlian et al., 2005) and the concentration of any soluble chemicals that may be introduced to the soil (Sauck, 2000; Georgaki et al., 2008) such as CO<sub>2</sub> gas (Zhou et al., 2012). The soil temperature generally has a smaller effect on soil EC than do VWC and exogenous chemicals (Grellier et al., 2006; Zhou et al., 2012). The EC of electrolytic solutions is dependent on the concentration, charge, and mobility of the ions in solution (Coury, 1999; Singha et al., 2011). Mobility is further dependent on temperature and the viscosity of the solvent (Coury, 1999). The concentration of one ion species can affect the concentration of other species, causing ions to dissolve or precipitate out of solution (Kharaka et al., 2010).

The CO<sub>2</sub> gas dissolves in water at atmospheric pressure and ambient temperatures typically present on the earth's surface (England

et al., 2011). Once dissolved, most of the CO<sub>2</sub> in aqueous solution exists as molecular CO<sub>2</sub>. Only a relatively small amount of the dissolved CO<sub>2</sub> reacts with water to form carbonic acid (Langmuir, 1997). Neither aqueous CO<sub>2</sub> nor carbonic acid is charged, so neither can act as a charge carrier for electric conduction. Carbonic acid will dissociate into a negative bicarbonate ion and a positive hydrogen ion in water of neutral pH. The bicarbonate ion will further dissociate into a negative carbonate ion and an additional positive hydrogen ion, but this reaction only causes significant concentrations of carbonate in more alkaline solutions (Andersen, 2002). These ions can act as a vector of charges for electric current formation if a voltage is applied to the carbonic acid solution.

The EC of an electrolytic solution depends not only on the concentration of ions, but also on the charge and mobility of the individual species of ions (Coury, 1999). The most significant cation present in a CO<sub>2</sub> solution is hydronium (H<sub>3</sub>O<sup>+</sup> or H<sup>+</sup>) that interacts with water to form various hydrogen bonded complexes, which include Zundel bonds, but it is unclear how well Zundel cations (and the more complex bonds) and others carry a charge. The value of pH, a measure of H<sup>+</sup> concentrations, has a role in EC, as a charge carrier and as a control on other ion concentrations. Kharaka et al. (2010) find that during the 2008 CO<sub>2</sub> release experiment at ZERT, the pH of the groundwater dropped from 7.04 before release to a minimum of 5.74 during release.

The electric current flow in electrolytic solutions is much like fluid flow. The more constrained the passages of flow are, the lower the EC will be (Berg, 2012). The geometry of a soil's solid phase is usually complex, and much has been made about constructing mathematical models around spheres, spheroids, and other shapes for the lattice structures (Banisi et al., 1993). Most geophysical models attempt to simplify this, often treating geometry as a single factor or constant. Within the EC of soils and rocks, the complex factors within the geometry of the soil structure are often simplified to a combination of porosity and tortuosity (Glover, 2009; Berg, 2012).

The objective of this paper is to develop a deterministic model to forecast the soil EC in response to possible leakage above CO<sub>2</sub> storage sites and to better understand the processes and conditions by which leaked CO<sub>2</sub> impacts the EC of the medium (soil or rock). The paper is organized as follows: the Introduction is followed by model formulation, in which the physical and chemical processes will be discussed. A sensitivity study of the model is then given, followed by application of the model to the observations in two field sites, where controlled CO<sub>2</sub> release experiments were carried out. A discussion and the conclusions are given in the last section.

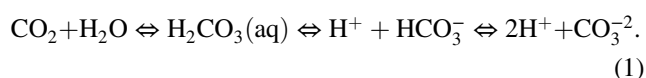
## MODEL FORMULATION

As CO<sub>2</sub> is leaked from subsurface storage, a series of physical-chemical processes that are relevant to change in the soil EC takes place: CO<sub>2</sub> gas dissolution in the groundwater and water in soil (Yan et al., 2011; Ziabakhsh-Ganji and Kooi, 2012), followed by dissociation of aqueous CO<sub>2</sub> into the ions, an increase in ions, and enhancement in the electrolyte conductivity of liquid water content in soil/rock (Wang et al., 2004; Singha et al., 2011) and thus the bulk soil/rock EC (Rhoades and Corwin, 1990). An analytical model will include all these factors to estimate bulk soil or porous rock EC from the CO<sub>2</sub> concentration, VWC, and temperature. Figure 1 shows the flowchart of the structure and procedures of the analytical model. The input data set includes the water content, temperature, and in situ CO<sub>2</sub> concentration. The temperature-dependent

CO<sub>2</sub> dissolution is then determined based on Henry's law. The dissolved CO<sub>2</sub> is in aqueous form. The dissociation constants of aqueous CO<sub>2</sub> are then calculated. These constants and the aqueous CO<sub>2</sub> concentration will be combined to determine the concentrations of bicarbonate and carbonate ions. Ionic concentrations are used to estimate fluid conductivity in soil or rocks. Archie's law is then used for the bulk soil/rock EC estimation. Finally, the bulk EC is adjusted for temperature. The model is calibrated using the exponents of saturation and cementation from Archie's law (Rein et al., 2004), and the chemical constant that will be discussed below as calibration constants. Validation of the model is done through comparison of the predicted to the EC data collected in the field. Additional validation is achieved by comparing the optimized calibration factors with those found in the literature and field data. The details of each model component are described below.

### Dissolution and dissociation

When CO<sub>2</sub> is leaked and passes through the water trapped in the pores of the soil or rock, it first dissolves in water-forming aqueous CO<sub>2</sub> and carbonic acid H<sub>2</sub>CO<sub>3</sub>. The aqueous H<sub>2</sub>CO<sub>3</sub>(aq) will dissociate into bicarbonate HCO<sub>3</sub><sup>-</sup> and hydrogen ions H<sup>+</sup>, and then into carbonate CO<sub>3</sub><sup>-2</sup> and H<sup>+</sup> ions. When CO<sub>2</sub> dissolves into water, most of it remains in an uncharged aqueous state (Langmuir, 1997). A small percentage of the aqueous CO<sub>2</sub> will react with the water and form carbonic acid. Carbonic acid will dissociate into derivative species bicarbonate and carbonate. The chemical equilibrium equation is shown below (Andersen, 2002):



The ionic species thus generated cause the solution to be more electrically conductive.

### Dissolution

The first step in determining the change in bulk soil EC due to CO<sub>2</sub> is to calculate how much CO<sub>2</sub> gas will dissolve in the water of soil. The greater the concentration or the greater the gas pressure of the CO<sub>2</sub>, the more of the gas will dissolve. Once dissolved, most aqueous CO<sub>2</sub> remains in the same molecular condition as it is in a gas; as a nonpolar, uncharged molecule. A small amount, less than 0.3%, will react with the water to form carbonic acid (Langmuir, 1997; Andersen, 2002).

Most equations dealing with the dissolution of CO<sub>2</sub> in water are at least partially derived from experimental solutions (Carroll et al., 1991). Dissolution can be calculated using the equation derived by William Henry, which allows us to calculate the amount of CO<sub>2</sub> that will dissolve at a particular pressure and temperature (Langmuir, 1997):

$$[\text{CO}_{2\text{aq}}] = P_{\text{CO}_2} \times K_0, \quad (2)$$

where brackets "[ ]" symbolize concentration,  $P_{\text{CO}_2}$  is the partial pressure of CO<sub>2</sub> that can be calculated by multiplying the volume concentration of CO<sub>2</sub> in the soil or rock by the atmospheric pressure. In particular  $P_{\text{CO}_2} = V_x p$ , where  $V_x$  is the volume of CO<sub>2</sub> gas divided by the total volume of gas and  $p$  is the total pressure. The value  $K_0$  is Henry's constant, in units of moles per liter per atmos-

phere pressure (mol/L/atm). Its dependence on temperature is given as (Mook, 2000)

$$pK_0 = -\log_{10} K_0 = \frac{-2622.38}{T} - 0.0178471T + 15.5873, \quad (3)$$

where and hereafter  $T$  is temperature in Kelvin.

### Dissolution and dissociation constants

The model requires two dissociation constants,  $K_1$  for bicarbonate and  $K_2$  for carbonate to calculate the concentration of carbonic acid species. Here, the Harned and Davis equations for  $K_0$  and  $K_1$  and the Harned and Scholes model for  $K_2$  are used (Mook, 2000). Associated with the dissolution of gas CO<sub>2</sub> in water (equation 1), the concentration of the dissolved CO<sub>2</sub> is given by

$$[\text{H}_2\text{CO}_3] = K_0 P_{\text{CO}_2}. \quad (4)$$

The dissociation of H<sub>2</sub>CO<sub>3</sub>(aq) in water occurs according to equation 1. The equations for the dissociation constants  $K_1$  and  $K_2$  are given as follows (Mook, 2000):

$$pK_1 = \frac{3404.71}{T} + 0.032786T - 14.8435, \quad (5)$$

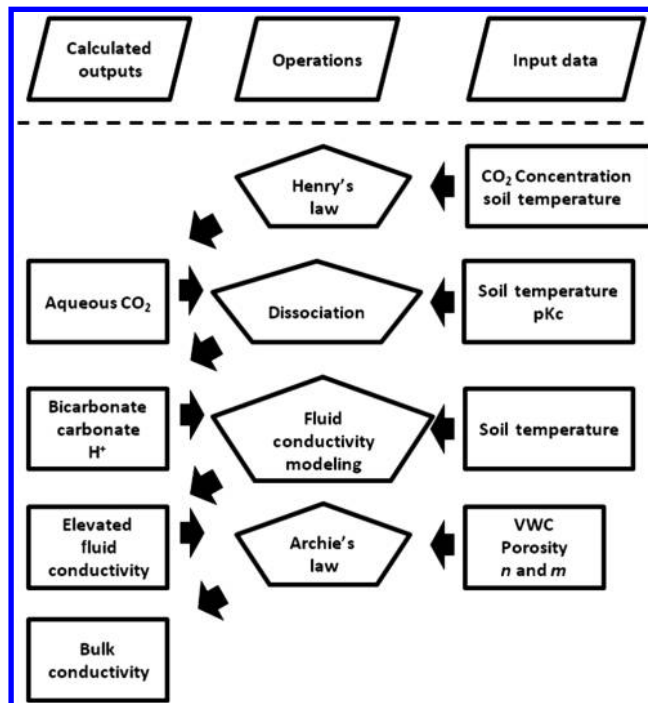


Figure 1. Flowchart of the model structure and procedure. The center column is the model processes (operations). The right column is the a priori data that are needed in each step. The left column is the model outputs of each step. The final output is the soil/rock EC and the inputs include soil CO<sub>2</sub> concentration, soil VWC, and soil temperature.

$$pK_2 = \frac{2902.39}{T} + 0.02379T - 6.4980. \quad (6)$$

For clarification on the use of dissolution constants,  $pK = -\log_{10}(K)$ , where  $p$  signifies an exponent of 10 in the literature.

## Dissociation

At atmospheric pressure and normal temperatures when  $\text{CO}_2$  gas dissolves in water, most of the gas enters an aqueous state where it remains as molecular  $\text{CO}_2$ . A small portion (0.26% of the carbonic acid at 25°C) of the aqueous  $\text{CO}_2$  reacts with water to form carbonic acid ( $\text{H}_2\text{CO}_3$ ) (Langmuir, 1997). Carbonic acid can dissociate into constituent ions depending on the pH of the solution. These concentrations are calculated as

$$[\text{HCO}_3^-] = \frac{[\text{H}_2\text{CO}_3]K_1}{K_c}, \quad (7)$$

$$[\text{CO}_3^{2-}] = \frac{[\text{HCO}_3^-]K_2}{K_c}. \quad (8)$$

Here, we introduced a new parameter  $K_c = 10^{-pKc}$ , where  $pKc$  is referred to as the chemical constant, to replace the concentration of hydrogen ion  $[\text{H}^+]$  within the ionic concentration calculations (equations 7 and 8) (Andersen, 2002). The chemical constant  $pKc$  not only includes the  $[\text{H}^+]$  generated by the carbonate chemical reactions  $\text{H}_2\text{CO}_3 \rightleftharpoons \text{H}^+ + \text{HCO}_3^-$  and  $\text{HCO}_3^- \rightleftharpoons \text{H}^+ + \text{HCO}_3^{2-}$ , but also the effects of buffering that decreases  $[\text{H}^+]$  and dissolution and/or precipitation of other ion species (e.g., minerals dissolution that increases  $[\text{H}^+]$ ) from the soil matrix, i.e.,  $pKc = \text{pH} + \text{chemical buffering} + \text{mineral dissolution/precipitation} + \text{cation exchange constants}$ , etc. Soil is a complex system that often contains chemical buffers that can change the equilibrium and reaction rates of acids (Langmuir, 1997). Factors of soil chemistry outside of  $\text{CO}_2$  dissolution and carbonic acid dissociation were abstracted to the chemistry coefficient. Usually, it is difficult to have an explicit expression for  $pKc$  because of the usually unknown number and types of dissolved ion species and chemical processes in the soil of an actual field site. However, once chemical processes reach equilibrium, for instance  $\text{CO}_2$  leakage with a relatively stable leaking rate, the chemical constant can be calibrated (see below). Thus, within a time scale greater than the relaxation time (the time taken for the chemical process to reach equilibrium), compared with changes in the VWC and  $\text{CO}_2$  due to leakage, other effects are much more stable. Therefore, the impact due to other factors on soil/rock EC is ignored when the impact due to VWC and soil  $\text{CO}_2$  is considered. The soil bulk EC is determined by a whole suite of factors, such as ion concentration, number of charges and mobility of ions species, porosity, and degree of saturation, etc., which we will discuss in the following sections.

## Fluid electric conductivity

Liquid water in soil or rock is treated as an electrolytic solution. The ions of this solution act as the charge carriers for the electric current formation when voltage is applied across the fluid. Specifically, when a potential difference is applied, it generates an electric field that mobilizes the ions in the solution. The ability of these ions

to carry a current depends on their charge, mass, and mobility (Coury, 1999; Singha et al., 2011). The greater the charge of an ion of the same mass, the greater the force that is exerted by the same electric field, causing it to move through solution more quickly. Counter to that force is the particle's inertia, the viscosity of the solution, and the difficulty of fluid flow through the soil or rock matrix (Berg, 2012). Mobility depends on the nature of the ion and its solvent. In particular, mobility depends on the ion's solvated radius, the viscosity of the solvent, and the charge of the ion. The solution's viscosity will affect the mobility of the ions with more viscous solutions impeding ionic movement and reducing the EC of the solution as a whole.

McCleskey et al. (2012) propose a method for calculating the EC of natural waters that incorporates a set of equations derived from measurements to calculate the ionic molal conductivities of ion species found in natural waters. The speciated concentrations are calculated using geochemical speciation models. Visconti et al. (2010) evaluate six different equations with 12 options of ion concentration (analytical concentration, free-ion concentration, or ionic activity) for EC calculation of soil solution at 25°C. The equation based on a linear relationship between EC and free-ion concentrations and ion pairs ultimately gave the best predictions. The fluid EC of liquid water in soil or rock when  $\text{CO}_2$  is dissolved and dissociated into ions is approximated by Kohlrausch's law in the form used in Coury (1999). It is the product of number of basic charges, ion concentration and mobility summed for each ion species, then multiplied by the Faraday constant  $F$ , as shown in equation 9. Mobility is a factor that takes into account the viscosity and hydrated radius of the ion to determine how much the solvent will impede the movement of the ion moving through it. The elevated fluid EC due to elevated soil/rock  $\text{CO}_2$  concentration during  $\text{CO}_2$  release or leakage is given as (Coury, 1999)

$$\sigma_{\text{CO}_2} = F \sum |z_i| u_i C_i, \quad (9)$$

where  $F$  is the Faraday constant ( $= 96485 \text{ C/mol}$ ),  $z_i$  the number of basic charges on an ion of the  $i$ th species,  $C_i$  the concentration of the  $i$ th ion type in  $\text{mol/m}^3$ . The  $u_i$  is the mobility of the  $i$ th ion species in units of  $\text{C} \cdot \text{s/kg}$ , defining the resistance the ion will experience in moving through the solvent and is given by (Coury, 1999)

$$u_i = \frac{|z_i|e}{6\pi\eta R_i}, \quad (10)$$

where  $e$  ( $= 1.602176565 \times 10^{-19} \text{ C}$ ) is the elementary charge and  $\eta$  is the viscosity of soil water that is  $1.002 \text{ mPa} \cdot \text{s}$  or  $0.001002 \text{ kg/(s} \cdot \text{m)}$  at 20°C (Kestin et al., 1978). The  $R_i$  is the solvated radius of the  $i$ th ion species in meters. Because water is a polar molecule, the charged ion attracts water molecules. These attracted  $\text{H}_2\text{O}$  molecules form a shell around the ion. The solvated radius is the mean radius of the ion in solution and the associated water molecules. The larger the solvated radius, the less mobile the ion will be, and subsequently, the lower the EC the solution will have. The solvated radius is estimated by (Gomaa and Al-Jahdalli, 2012)

$$R_i = \left( \frac{3V}{4N_A\pi} \right)^{1/3}, \quad (11)$$

where  $N_A$  is Avogadro's number ( $= 6.023 \times 10^{23}$ ),  $V$  is the molar volume in  $\text{cm}^3/\text{mol}$  that is a temperature dependent parameter and can be estimated for CO<sub>2</sub> as (Enick and Klara, 1990)

$$V = 1799.36 - 17.8218T + 0.0659297T^2 - 1.05786 \times 10^{-4}T^3 + 6.200275 \times 10^{-8}T^4. \quad (12)$$

Another factor that may affect the EC of concentrated electrolytes is association. *Association* is the attraction of two oppositely charged ions. As the ionic concentration increases, the probability that two oppositely charged ions will come into contact and attract or deflect also increases (Barta, 1982; Dickinson et al., 2011). This causes interference and a decrease in fluid EC. However, given the low salinity of the liquid water in soil or rock and the very small amount of CO<sub>2</sub> that dissolves and dissociates, it is unlikely to be a significant factor in limiting the fluid EC. This is supported by the field data of Kharaka et al. (2010) at the ZERT site. Thus, we ignore the effect of association.

### Bulk soil EC and moisture dependence

The bulk EC of a soil or porous rock depends on the VWC and its electrolytic EC contained within the pore spaces, the space availability, and the permeability and EC of the soil matrix. To predict bulk EC, it is necessary to know or estimate the porosity of the soil and the VWC by the conducting fluid.

Soil or porous rock is composed of particles with spaces (pores) that are often filled with air and water. Air is almost completely resistive because the EC of air is effectively zero. The EC of the solid phase depends on the mineralogy of the soil or rock; silica sands tend to have very low conductivity, whereas clays and shales have high conductivity (Samouëlian et al., 2005). The ZERT site topsoil is sandy silt transitioning downward to gravel; well logs from before the experiment classified the top 40 cm of the site as silt, sand, and gravel. The CO<sub>2</sub> vadose zone is solid limestone with 98% CaCO<sub>3</sub> content, according to Loisy et al. (2013). Thus, the fluid EC should dominate most soil and rock EC measurements at these two sites (Bigalke, 2000). Another consideration of the matrix of water and soil particles is how much of the pore space is occupied by water. The more the pore space is filled with water, the greater the EC of the soil as a whole.

Archie's law is used to determine the EC of porous rocks or soil filled in with conductive fluid. It takes into account the porosity of the rock and the level of saturation. The basic form of the law is the fluid EC multiplied by the porosity (to the power of the cementation exponent) multiplied by the saturation (to the power of the saturation exponent). Archie's law assumes that the solid media's EC is negligible. This assumption does not hold in shales, rocks, and soils with high clay content. Archie's law, as it commonly appears in the literature (Rein et al., 2004; Friedman, 2005), is

$$\sigma_{ps} = \sigma_f P^m S_w^n, \quad (13)$$

where  $\sigma_{ps}$  is the EC of partly saturated soil or porous rock;  $\sigma_f$  is the fluid EC, which will be explained in the next section;  $P$  is the porosity; and  $m$  is the cementation exponent and is a geometrically controlled term (Glover, 2009). The value  $S_w$  is the degree of saturation

defined as the water content of the soil divided by the porosity  $P$  and  $n$  is the saturation exponent and it weights VWC. The version of Archie's law used here is sometimes referred to as the extended Archie's law (Friedman, 2005). The cementation factor  $m$  and the saturation coefficient  $n$  are ambiguous parameters. There are some debates as to the physical nature of these exponents (Friedman, 2005; Glover, 2009; Berg, 2012), but there is no consensus yet (Laloy et al., 2011). Tortuosity is a way of quantifying the ease of flow by comparing the actual travel length and the straight line length (Bristow et al., 2001; Berg, 2012); thus, Glover (2009) interprets the cementation exponent as an analog to tortuosity. Some researchers take the cementation and saturation coefficients ( $m$  and  $n$ ) as calibration parameters, whereas others attempt to subscribe physical attributes to them (Friedman, 2005; Glover, 2009). Here, we will take the two parameters ( $m$  and  $n$ ) and the chemical constant  $pKc$  as the site calibration parameters. Whether the calibrated values are within the commonly accepted values in the literature should be a good test to determine if the model works well. Because these parameters are difficult to measure in situ and are not easily available for a specific site, they are estimated by tuning the model prediction to the EC measured. Specifically, the values of these parameters are changed and the rms between the modeled and observed soil EC is calculated. The set of the values of these parameters that results in the minimum rms is selected.

### Ambient electric conductivity

The soil EC measured before CO<sub>2</sub> release (or leakage) is defined as the ambient soil EC. *Ambient soil EC* is defined as the soil EC due to factors including VWC other than injected CO<sub>2</sub>. The ambient soil EC is caused by the ions present in the soil VWC and clay if present in the EC before or after CO<sub>2</sub> release. However, we assume the clay content in the soil is not changed during CO<sub>2</sub> release or leakage, so that soil EC change above the ambient value is due to just the released or leaked CO<sub>2</sub>. Although ambient CO<sub>2</sub> can generally be defined as average global atmospheric concentration that can increase to more than 800 ppmv (ppm by volume) by the end of this century if no mitigation action is taken (Thomson et al., 2014), there is large local variability (Longinelli et al., 2013) that must be taken into account. To consider the variation of the ambient soil CO<sub>2</sub> concentration due to respiration of soil microbes and vegetation roots (Zhou et al., 2013), we have developed an algorithm that automatically separates CO<sub>2</sub> concentration data recorded into low and high groups that correspond to ambient and leakage scenarios, respectively, by picking up data points of less than 5% of the maximum as the ambient values, so that the algorithm works for sites of completely different CO<sub>2</sub> levels. This is 5% of the maximum CO<sub>2</sub> concentration measured at a site (including the ambient and leaking periods), not 5% absolute CO<sub>2</sub> concentration. This percentage value as a threshold can be adjusted if only the average value of the ambient CO<sub>2</sub> concentration is less than this threshold multiplying the average value of the CO<sub>2</sub> concentration during leakage. Fortunately, due to the very large difference between the ambient values and the leaking values, almost no difference was found for other threshold values more than 5% as tested using the data sets at the two field sites described below. We use a percentage for a threshold, so the algorithm works for sites of completely different CO<sub>2</sub> levels. For instance, at the ZERT site, the measured soil CO<sub>2</sub> concentration (gas) varied from the mean background CO<sub>2</sub> level of 0.63% before CO<sub>2</sub> release to greater than 20% during the CO<sub>2</sub> release (Zhou et al.,

2012), whereas at the CO<sub>2</sub>-Vadose Project site, the measured rock CO<sub>2</sub> concentration (gas) varied from the mean background value of approximately 400 ppm before CO<sub>2</sub> release to approximately 600,000 ppm during CO<sub>2</sub> release (Le Roux et al., 2013). For the measurement method of soil/rock gas CO<sub>2</sub> concentration, please see Zhou et al. (2012) and Le Roux et al. (2013). For the time points that had CO<sub>2</sub> concentration below the threshold the EC averaged to give the ambient bulk conductivity of the soil.

The ambient fluid EC of the soil or rock can be inverted using Archie's law to give

$$\sigma_a = \sigma_{ps0} P^{-m} S_w^{-n}, \quad (14)$$

where  $\sigma_a$  is the ambient fluid EC within soil/rock in units of decisiemens per meter (1 dS/m = 0.1S/m) when there is no CO<sub>2</sub> release or leakage. The elevated fluid EC due to CO<sub>2</sub> released/leaked (equation 9) is due to various charges caused by the dissolution and dissociation of the elevated soil or rock CO<sub>2</sub> concentration during CO<sub>2</sub> release or leakage. We assume that the increased fluid EC due to the released (or leaked) CO<sub>2</sub> can be superimposed onto the ambient fluid EC. This assumption is consistent with the linear relationship between the predicted soil EC and soil CO<sub>2</sub> concentration as shown in the next subsection (see Figure 2). The overall fluid EC of the pore water in soil/rock during CO<sub>2</sub> release or leakage is thus the sum (see equation 9) of the ambient fluid EC ( $\sigma_a$ ) and the elevated fluid EC due to CO<sub>2</sub> ( $\sigma_{CO_2}$ )

$$\sigma_f = \sigma_a + \sigma_{CO_2}. \quad (15)$$

### MODEL SENSITIVITY STUDY

Sensitivity analysis was conducted to study the response of the model output (soil bulk EC) to model input parameters, such as soil

CO<sub>2</sub> concentration, VWC, and soil temperature. In the following sensitivity analysis,  $m$  and  $n$  are held at 2.0.

#### EC versus CO<sub>2</sub>

Figure 2 shows the model's predicted EC versus CO<sub>2</sub> concentration. Figure 2a shows the VWC at 0.25 m<sup>3</sup>/m<sup>3</sup> and soil temperature at 4°C, 8°C, and 12°C; Figure 2b shows the temperature at 15°C and the soil/rock liquid water content varying from 0 to 0.4 m<sup>3</sup>/m<sup>3</sup> at an interval of 0.1 m<sup>3</sup>/m<sup>3</sup>. For both cases, the chemical constant  $pKc$  is 7.0. We can see that the soil/rock EC varies linearly with soil/rock CO<sub>2</sub> concentration. Because the larger the slope, the more sensitive the EC is to the CO<sub>2</sub> concentration; we concluded that the soil/rock EC is more sensitive to the soil/rock CO<sub>2</sub> concentration at lower soil/rock temperature and/or higher soil/rock moisture.

#### EC versus VWC

VWC is important to the EC of soil as it provides the medium for ions to dissolve and move. Figure 3 shows the soil/rock EC versus liquid water content in volume when the chemical constant  $pKc$  is held to be 7.0. Figure 3a shows the soil/rock temperature held at 15°C and the soil/rock CO<sub>2</sub> concentration at 4%, 12%, and 20%. We can see that the model output (soil/rock EC) increases nonlinearly with the increasing liquid water content for fixed temperature and CO<sub>2</sub> concentration. However, if we imagine a vertical line at a fixed value of water content intersecting the three curves corresponding to the different CO<sub>2</sub> concentration values, we will see that the slope at the intercepted point is larger for a higher CO<sub>2</sub> concentration. This means that the soil/rock EC is more sensitive to the soil/rock water content at higher CO<sub>2</sub> concentration when the temperature is held at a constant value. Figure 3b shows the CO<sub>2</sub> concentration at 10% and the soil/rock temperature varying from 4°C to 20°C with intervals of 4°C. The figure shows that the five curves corresponding to the five temperature values almost overlap. This demonstrates the

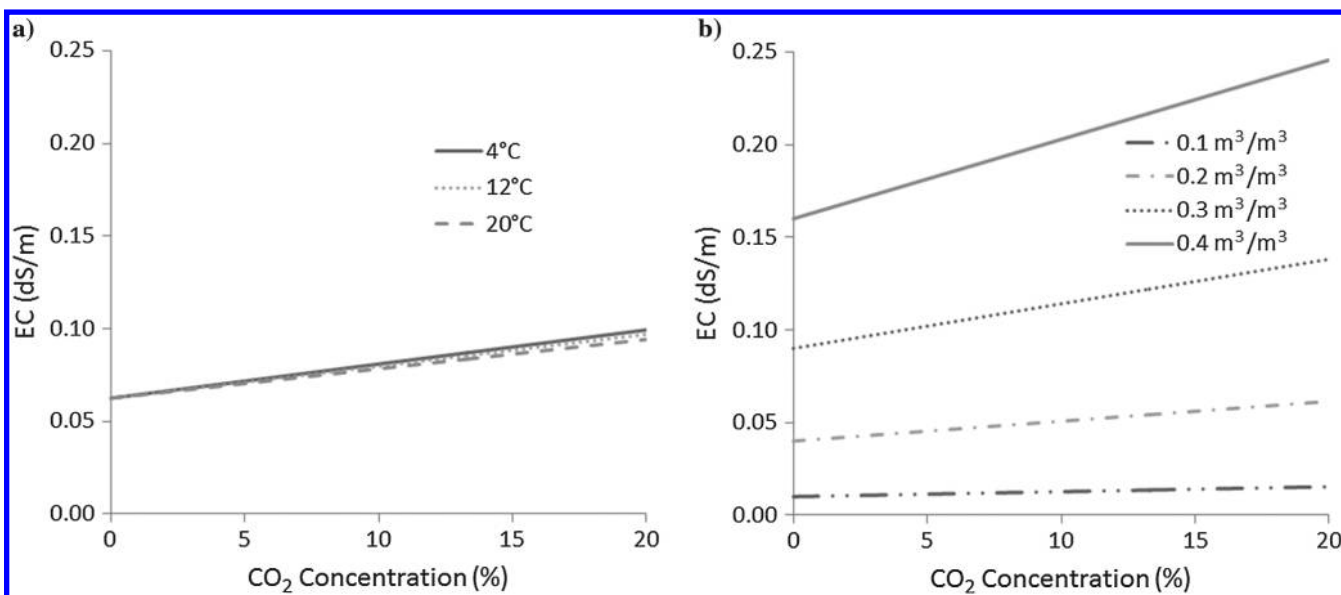


Figure 2. The model's sensitivity to CO<sub>2</sub> concentration. Panel (a) is for soil/rock moisture at 0.25 m<sup>3</sup>/m<sup>3</sup> and temperature at 4°C, 8°C, and 12°C. Panel (b) is for soil/rock temperature at 15°C and soil/rock water content varying from 0.1 to 0.4 m<sup>3</sup>/m<sup>3</sup> at an interval of 0.1 m<sup>3</sup>/m<sup>3</sup>. The results show that the soil EC is proportional to the soil CO<sub>2</sub> concentration when the soil temperature and soil VWC are fixed.

insensitivity of the relationship between the soil/rock EC and the soil/rock water content to the soil/rock temperature.

### EC versus soil temperature

Figure 4 shows the soil/rock EC versus the soil/rock temperature when the chemical constant  $pKc$  is held to be 7.0. Figure 4a shows

the soil/rock CO<sub>2</sub> concentration at 10% and water content varying from 0 to 0.4 m<sup>3</sup>/m<sup>3</sup> at an interval of 0.1 m<sup>3</sup>/m<sup>3</sup>. Figure 4b shows the soil/rock moisture held constant at 0.25 m<sup>3</sup>/m<sup>3</sup> and CO<sub>2</sub> concentration varying from 4% to 20% at an interval of 4%. From both panels, we can see that the soil/rock EC decreases with increasing temperature, given that CO<sub>2</sub> dissolves more readily in colder water than in warmer water. The effect of soil/rock temperature on EC is

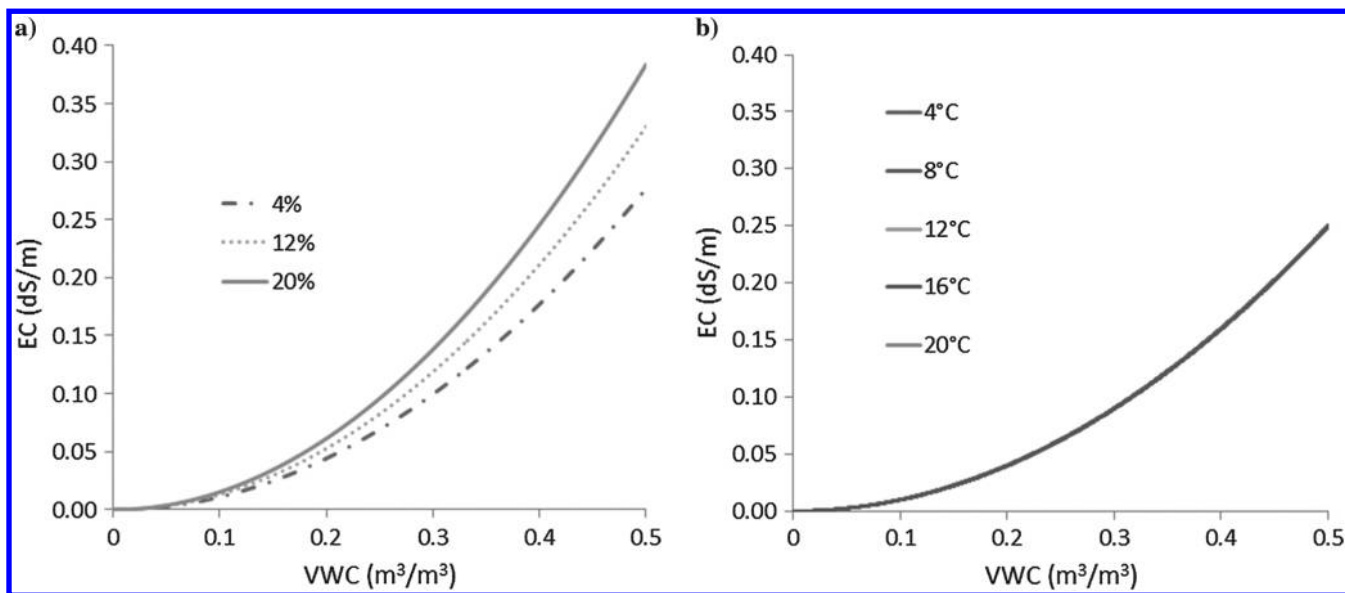


Figure 3. Sensitivity analysis of EC versus soil/rock water content. Panel (a) is for the temperature at 15°C and the soil/rock CO<sub>2</sub> concentration at 4%, 12%, and 20%. Panel (b) is for CO<sub>2</sub> concentration at 10% and the soil/rock temperature varying from 4°C to 20°C at an interval of 4°C. The results show that soil EC increases nonlinearly (exponentially) with the increase in soil VWC for a fixed soil temperature and soil CO<sub>2</sub> concentration. Because the effect of temperature within the temperature range that we met in the field is very small compared with the VWC, all traces in panel (b) overlap.

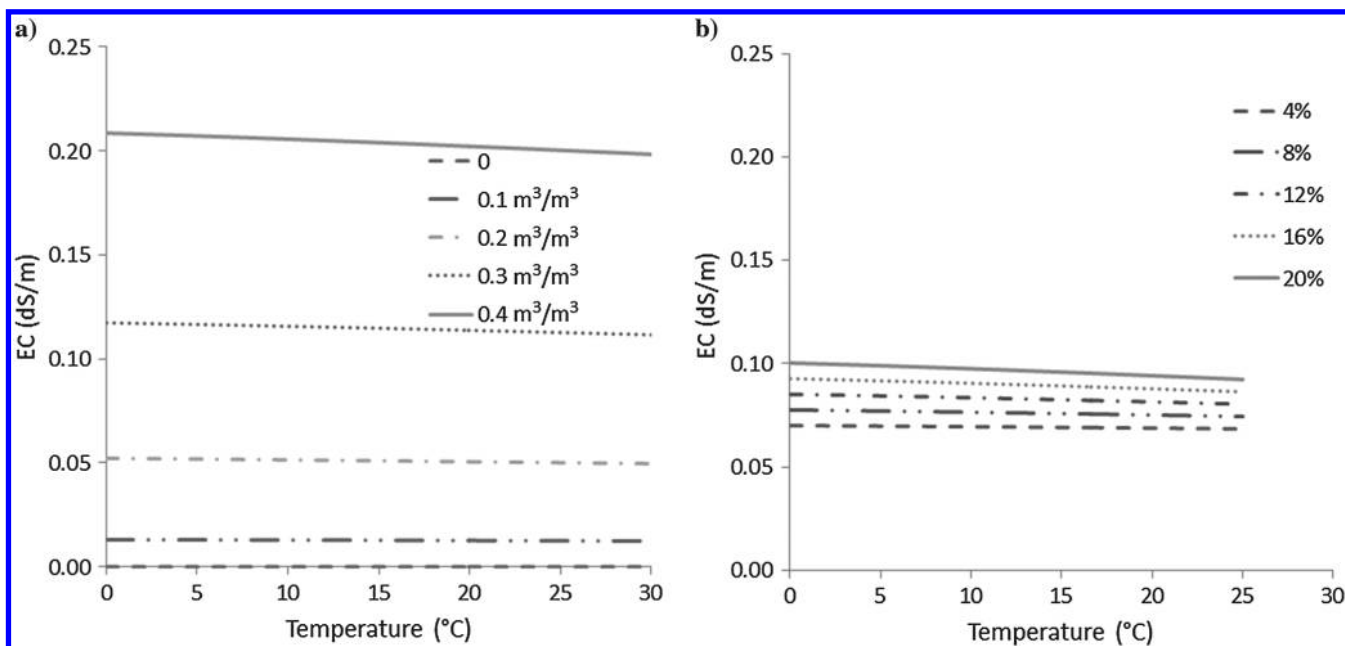


Figure 4. The model's sensitivity of soil/rock EC to soil temperature. Panel (a) is for CO<sub>2</sub> concentration held constant at 10% and soil/rock moisture varying from 0 to 0.4 m<sup>3</sup>/m<sup>3</sup> at an interval of 0.1 m<sup>3</sup>/m<sup>3</sup>. Panel (b) is for VWC held constant at 0.25 m<sup>3</sup>/m<sup>3</sup> and CO<sub>2</sub> concentration varying from 4% to 20% at an interval of 4%. Results show that the soil EC decreases slowly with increasing soil temperature when the soil CO<sub>2</sub> concentration and soil VWC are fixed.

very mild: A 30°C change in temperature will produce less than a 0.01 dS/m change in bulk EC. However, the EC is more sensitive to temperature for higher CO<sub>2</sub> concentration and/or higher soil/rock water content.

### EC versus chemistry constant $pKc$

Figure 5 shows the model's sensitivity to the chemistry constant  $pKc$ . VWC is held at 0.25 m<sup>3</sup>/m<sup>3</sup>, the temperature is held at 15°C, and the CO<sub>2</sub> concentration is held at three levels, i.e., 0%, 12%, and 20%, respectively. The model output EC is not sensitive to changes in  $pKc$  when the soil CO<sub>2</sub> concentration is zero or when  $pKc$  is smaller than approximately 5.0 when the soil CO<sub>2</sub> concentration is above zero. However, the model output EC increases nonlinearly as the chemistry constant  $pKc$  increases when the soil CO<sub>2</sub> concentration is not zero. A large  $pKc$  value could mean either low buffering in the pore water or more ions that can be readily dissolved. From Figure 5, we can see that when there is CO<sub>2</sub> release or leakage, for pore water with an initial  $pKc$  of 8, carbonic acid formed from CO<sub>2</sub> dissolution will dissociate into proton and bicarbonate, increasing the fluid ionic strength, number of ions, and the soil EC. Subsequent decrease of  $pKc$  will reverse the dissociation process, reducing the ionic strength, number of free ions, and the surface charge density on the mineral surfaces, all of which decrease the soil EC. At the same time, a decrease of  $pKc$  from CO<sub>2</sub> dissolution can also change the mineral dissolution/precipitation and ion exchange processes and subsequently change the fluid conductivity (Dafflon et al., 2013).

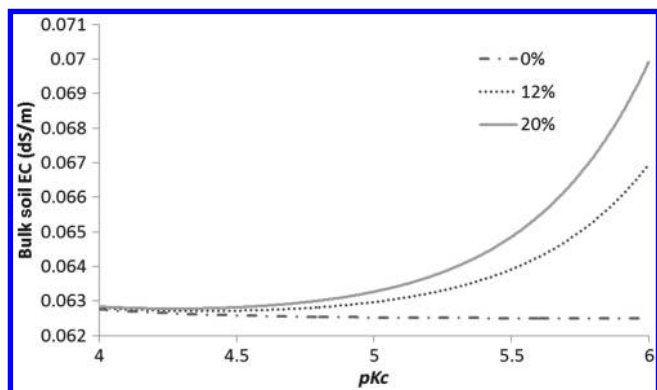


Figure 5. The model sensitivity of soil/rock EC to the chemistry constant,  $pKc$ . The soil moisture and soil temperature are 0.25 m<sup>3</sup>/m<sup>3</sup> and 15°C, respectively. The soil CO<sub>2</sub> concentration is at three levels, i.e., 0%, 12%, and 20%, respectively.

**Table 1. Times of CO<sub>2</sub> release experiments for years 2009–2011 at ZERT.**

Data set	2009	2010	2011
Start date	15 July, 12:00	19 July, 12:35	18 July, 12:16
End data	12 August, 12:00	15 August, 12:35	15 August, 12:00
Time interval	30 min	30 min	5 min
Samples ( <i>N</i> )	3441	3654	22,409

## CASE STUDY ONE: ZERT SITE

### Site description and data collected

To develop and test technologies for CO<sub>2</sub> leakage detection, a test site was built at the ZERT center in Bozeman, Montana, USA. A pipe slotted in six zones was buried at a depth of approximately 2 m below ground surface, with CO<sub>2</sub> pumped into each zone independently at slightly above atmospheric pressure and allowed to diffuse into the soil. At the ZERT site, the surface expression of CO<sub>2</sub> flux from the release was approximately 5 m wide above the pipe. However, the size of the hot spots should depend on the depth of the CO<sub>2</sub> injection and geology of the overlying rocks. Soil gas CO<sub>2</sub> measurement in the perpendicular direction to the pipe orientation showed that the soil gas CO<sub>2</sub> concentration 7 m away from the pipe was almost the same as the background value (Lakkaraju et al., 2010). Here, the soil gas CO<sub>2</sub> concentration is defined as the volumetric percentage of CO<sub>2</sub> gas in the soil atmosphere. We can see that at this specific site for an injection depth of 2 m, an area within a 7-m radius around the center of the leaking site is large enough for the monitoring of the release of CO<sub>2</sub>. A detailed characterization of the site was described by Spangler et al. (2009). Soil EC and other soil environmental data were observed at the ZERT site in the summer controlled-CO<sub>2</sub> release experiments in 2009, 2010, and 2011, following the method described by Zhou et al. (2012). Four sets of data were collected: soil CO<sub>2</sub> concentration, VWC, bulk soil EC, and temperature. Table 1 shows the starting and end times for CO<sub>2</sub> release for each year, the time interval for sampling, and the total number of data samples. The EC, temperature, and water content data were collected using Decagon 5TE probes buried within the vadose zone. These probes have a resolution of 0.01 dS/m for the range from 0 to 7 dS/m and a resolution of 0.05 dS/m for the range from 7 to 23.1 dS/m with an error of ±10%. Carbon dioxide gas concentrations were provided from ZERT. Zhou et al. (2012) show that the presence of CO<sub>2</sub> in soil causes a detectable increase in bulk soil EC.

Figure 6 shows the measured data from the 2011 summer CO<sub>2</sub> release experiment. In Figure 6a, CO<sub>2</sub> shows the sharp increase in the concentration of the gas within the soil after the release started. It also shows the diffusion of lower concentrations after the release was ended. The sudden drop in the soil CO<sub>2</sub> concentration during the CO<sub>2</sub> release (Figure 6a) is due to an outage of electricity caused by a lightning storm at approximately 9:47 p.m. on 11 August 2011. The CO<sub>2</sub> flow was back up at 6:08 a.m. on 12 August 2011. VWC (Figure 6c) shows the steady desiccation of the soil over the course of the summer, with no major storms adding water to the soil. The temperature data (Figure 6b) show the temporal evolution of soil temperature, with the diurnal swings still visible. It also shows the beginning of the cooling brought about by the end of the summer. The EC data (Figure 6d) show a sharp increase at the start of the CO<sub>2</sub> release, marked with the left vertical dashed line. However, the shut off of CO<sub>2</sub> (the date of the end of CO<sub>2</sub> release is marked by the right vertical line) is not as clear as the start due to the slow release of CO<sub>2</sub> trapped in the soil. The recorded soil EC shows a single large increase from approximately 0.35 dS/m to 0.50 dS/m on 18 July, when the CO<sub>2</sub> release started. Other than

this jump, the EC steadily decreases until staying steady at slightly less than 0.15 dS/m.

### Model calibration

Although the major inputs to the model (soil CO<sub>2</sub> concentration, water content, and temperature) are measured in the field, there are several factors that have to be estimated or derived from independent data sources. Soil bulk EC data collected at the ZERT site from 2009 to 2011 (see Table 1) are divided into two subsets: one for model calibration and others for validation. Field measurements taken in 2011 are used for model calibration. Measurements from 2009 and 2010 are used for validation.

The exponents of cementation and saturation are generally not available from field measurement and are thus used as tuning parameters. Their values are determined by using the least-squares method to find the best fit of the calculated soil EC to the measured data in 2011 at ZERT. In addition, the data from a control site are run to test the model's ability to work under normal conditions (no CO<sub>2</sub> leakage). For the value of the saturation exponent  $n$ , and the cementation exponent  $m$ , the literature shows a large range of variability. For instance, Laloy et al. (2011) indicate a range of 1–6 for the cementation exponent and 1–4 for the saturation exponent.

Glover (2009) finds that the saturation exponent varies from 1.5 to 2.5, and the cementation exponent varies from 1 to 5. Friedman (2005) indicates a range of 1.3–4.4 for the cementation exponent. Rein et al. (2004) state that the saturation exponent is often assumed to be two, whereas the cementation exponent is 1.3 for unconsolidated sediments. The third calibration parameter is the soil chemistry coefficient.

The data are divided into two sets depending on whether the soil CO<sub>2</sub> concentration is ambient or due to CO<sub>2</sub> release (Figure 6). The set of data that corresponds to the released CO<sub>2</sub>, where the soil CO<sub>2</sub> concentration is much higher than ambient, is used to calibrate for  $m$ ,  $n$ , and  $pKc$ . Calibration is performed through best fitting the observed soil EC data with minimum rms error. The best-fit value of the cementation exponent is  $m = 1.95$ , and that of the saturation exponent is  $n = 3.15$  at the ZERT site, both of which lie within the range of accepted values. The saturation and cementation exponents calibrated are then applied to the ambient data set, which is then calibrated for  $pKc$ . The result is  $pKc = 4.7$ . From Figure 5 we may see that soil EC is not very sensitive to  $pKc$ . However, from equations 7–9, we can see that the soil EC depends on ion concentrations of bicarbonate and carbonate, both depending on the concentration of the dissolved CO<sub>2</sub> and  $pKc$ . The concentration of the dissolved CO<sub>2</sub>

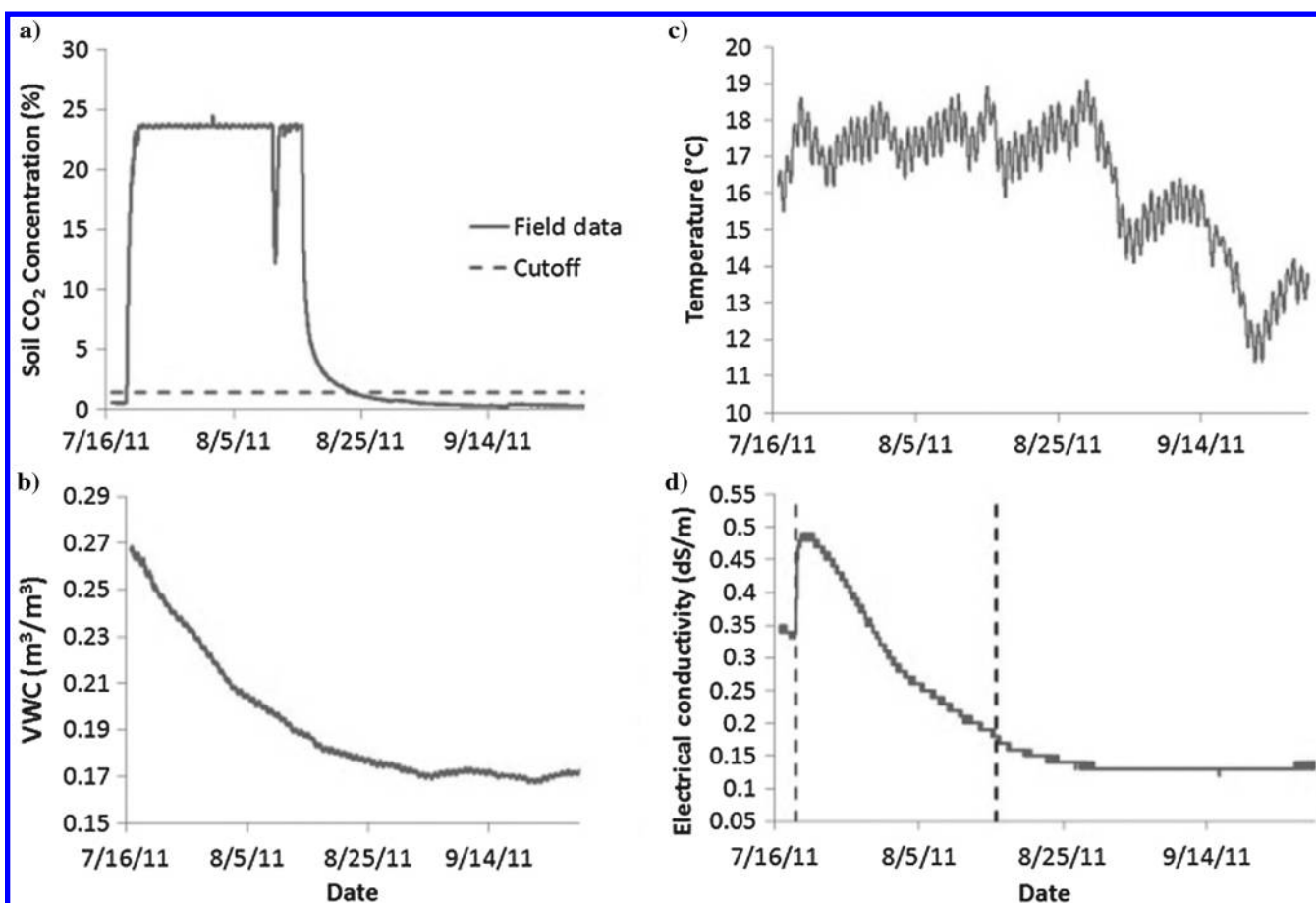


Figure 6. Time series of measurement of (a) soil CO<sub>2</sub> concentration, (b) soil VCW, (c) soil temperature, and (d) soil EC in 2011, summarized in Table 2. The two vertical dashed lines in panel (d) indicate the starting and ending times of the CO<sub>2</sub> release. The CO<sub>2</sub> concentration contains the calibration cutoff, where the data set is broken into two parts: ambient CO<sub>2</sub> and release CO<sub>2</sub>. The sudden drop in the soil CO<sub>2</sub> concentration during the CO<sub>2</sub> release (panel a) is due to an outage of electricity caused by a lightning storm at approximately 9:47 p.m. on 11 August 2011. CO<sub>2</sub> flow was back up at 6:08 a.m. on 12 August 2011.

increases rapidly during the CO<sub>2</sub> release. The impact on the soil EC due to the increase of the concentration of the dissolved CO<sub>2</sub> may dominate the impact due to the change in  $pKc$ .

Figure 7 shows the comparison of the calculated soil EC using the present model with the calibrated values for  $m$ ,  $n$ , and  $pKc$ . As ex-

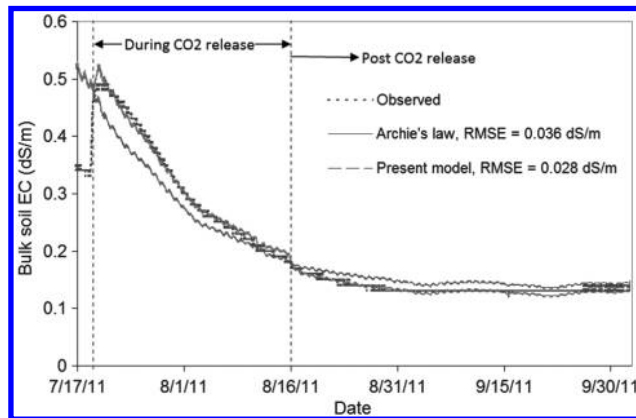


Figure 7. Comparison of the soil EC observed at the ZERT site and that generated by the present model and just Archie's law. The time period for the CO<sub>2</sub> release is indicated by the vertical dashed lines. Both models can predict the general trend of the observation, but Archie's law underestimates the observation during the CO<sub>2</sub> release and overestimates the observation after CO<sub>2</sub> release. The present model agrees better with the measurement than Archie's law for during and after periods of time. Neither model, however, agreed with the observation during the short prerelease period.

pected, the calculated and measured bulk soil conductivities agree well with each other, with rms error being 0.028 dS/m. To see the difference between the present model and Archie's law (equation 13) in predicting the soil EC, we added the fitting to the observation using Archie's law in Figure 7. The predicted soil EC using Archie's law is independent of the carbon dioxide level; the tuning parameters were  $n = 2.90$ ,  $m = 2.00$ , and  $\sigma_f = 9.3$ . Here, the same approach, i.e., minimizing the misfit between the modeled and observed soil bulk EC during calibration, was used to obtain the tuning parameters. During the CO<sub>2</sub> release, Archie's law underestimated the soil EC compared with the observation, whereas after CO<sub>2</sub> release, Archie's law overestimated the soil EC. The overall rms error was 0.0364 dS/m. For both models, the largest discrepancy is before the CO<sub>2</sub> release, where both models overestimate the EC. Two causes may contribute to the fact that the modeled EC does not fit the measured bulk EC before injection: (1) both models are static analytical models and a dynamic model may be necessary to model a sudden change, and (2) the observation period of time for prerelease is too short to obtain statistically significant results. However, the much longer period after release may compensate for the short prerelease.

### Model validation

Once the model is calibrated using the 2011 data set, it can be used to predict the EC values for 2009 and 2010. The effectiveness of the prediction capacity can be validated through comparison with measurement. Figure 8 shows measured data from the 2009 summer CO<sub>2</sub> release experiment, including the time series of soil CO<sub>2</sub> concentration

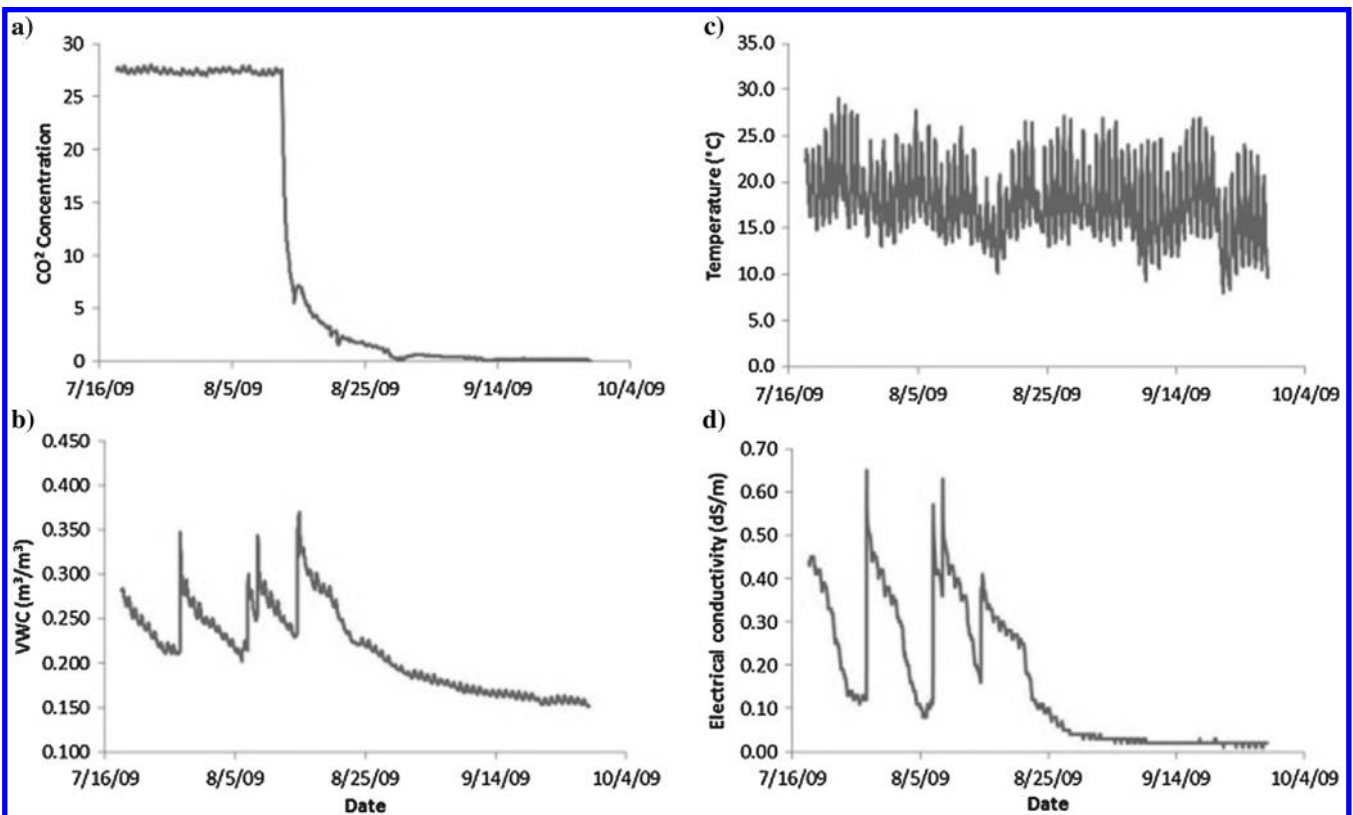


Figure 8. Time series of (a) soil CO<sub>2</sub> concentration, (b) soil VCW, (c) soil temperature, and (d) soil EC from the 2009 summer CO<sub>2</sub> release experiment.

(Figure 8a), soil temperature (Figure 8b), soil VCW (Figure 8c), and soil EC (Figure 8d). The data collection started during the CO<sub>2</sub> release. There were several large rainstorms causing large increases in the VWC. The dominant effect of the soil VWC is visible when comparing the sudden increase of the soil EC in response to the sudden increase in soil VWC corresponding to each storm. However, the decrease of the soil EC in response to the decrease in soil CO<sub>2</sub> concentration after the CO<sub>2</sub> release was terminated on 13 August 2009 is also visible but entangled with the impact due to the decrease in the soil VWC.

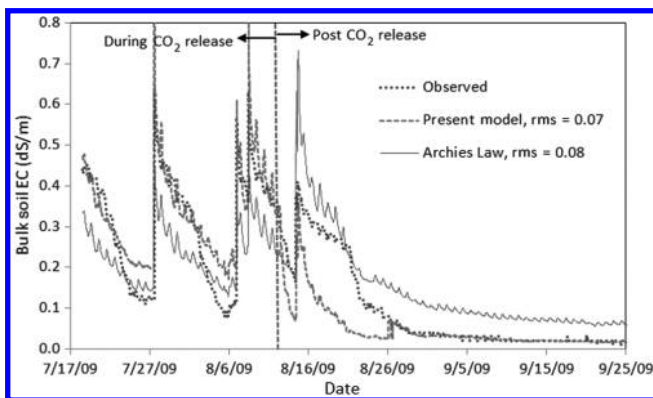


Figure 9. The bulk soil EC data from the 2009 release experiment and the model prediction. The model predictions can generally recover the trend of the observed time series of soil EC with rms error = 0.07 dS/m for the present model and with rms error = 0.08 dS/m for Archie's law.

Figure 9 shows the comparison of the modeled and observed soil EC values for year 2009. It should be noted that data collection started after the CO<sub>2</sub> release had begun. The end of the release is marked by the vertical dashed line. There were several rainstorms during this year, and the rapid increases in the soil EC due to the storms were clearly visible (Zhou et al., 2012). The same calibrated values  $m = 1.95$ ,  $n = 3.15$  as in Figure 7 (for the year 2011) were used. However,  $pKc$  needs to be calibrated because the CO<sub>2</sub> release rate is different from 2010. The calibrated  $pKc$  value is 5.7 for data of the background CO<sub>2</sub> level after release (see Zhou et al., 2012) and 5.3 for during CO<sub>2</sub> release. The present model correctly estimates the maximums in the EC during release, but overestimates the minimums by some 0.1 dS/m. The rms error is 0.07 dS/m. The predicted soil EC using Archie's law is independent of the carbon dioxide level; the same calibrated parameters  $n = 2.90$  and  $m = 2.00$  as in Figure 7 were used. Similarly,  $\sigma_f$  needs to be calibrated because of the different CO<sub>2</sub> release rate, the newly calibrated  $\sigma_f$  is 5.1. Compared with the measurement, Archie's law can also predict the soil EC well, but compared with the present model, the rms error from Archie's law is higher (0.08 versus 0.07). During the first couple of days after CO<sub>2</sub> release, Archie's law predicted better than the present model; otherwise, the present model predicts better. Because the model of this study takes into account the CO<sub>2</sub> impact on soil EC and it is based on chemical equilibrium, dynamic behavior due to a sudden change in CO<sub>2</sub> may result in a larger error compared with stable or quasi-stable situations.

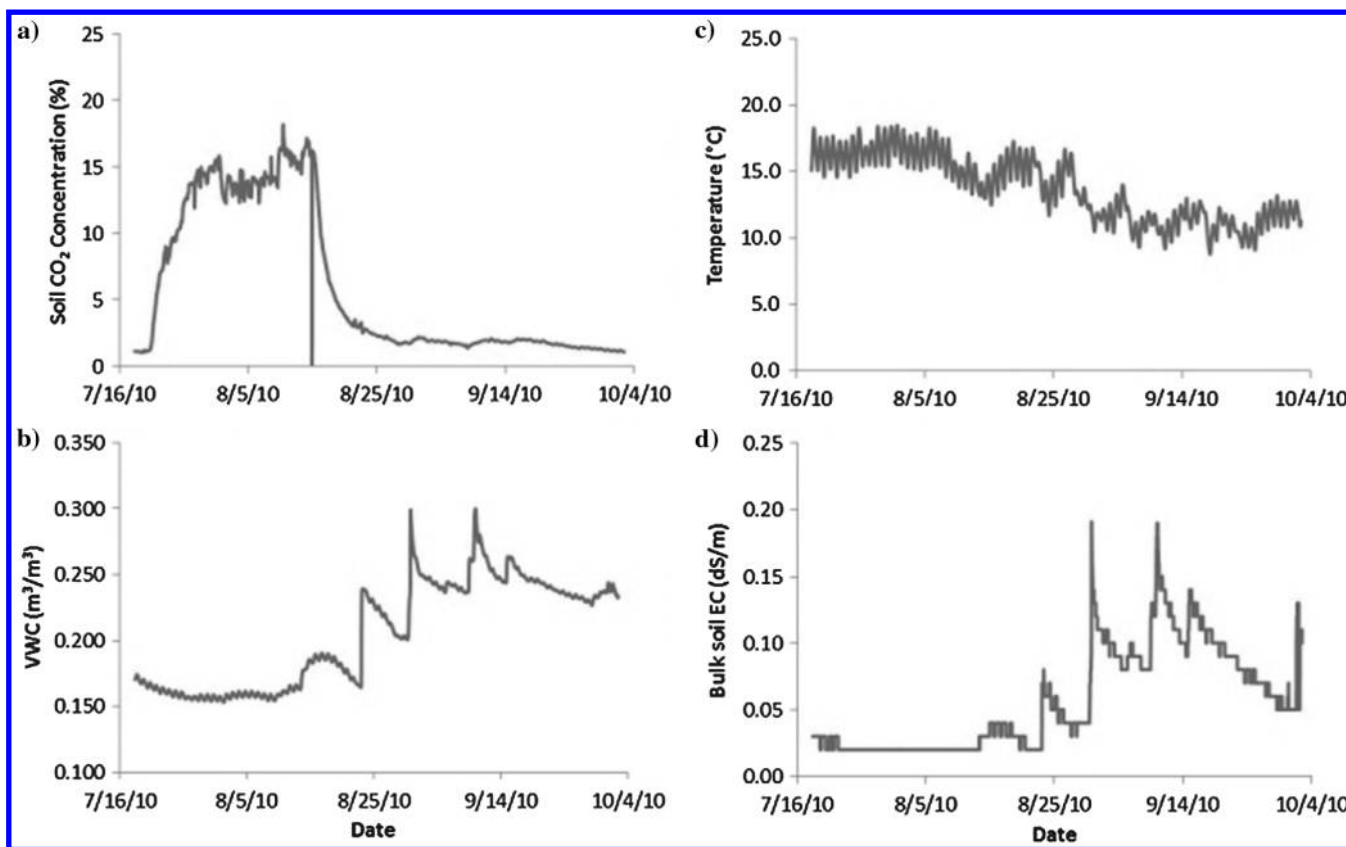


Figure 10. Summary of the ZERT 2010 field data. During the CO<sub>2</sub> release, the soil VWC was low ( $< 0.2 \text{ m}^3/\text{m}^3$ ), and the observed soil EC during the CO<sub>2</sub> release with large precipitation events occurred only after the gas had been cut off.

Figure 10 shows the field data at the ZERT site from the summer CO<sub>2</sub> release in 2010, which is similar to that in Figure 8 for the summer CO<sub>2</sub> release in 2009. The sudden decrease of soil CO<sub>2</sub> concentration to almost zero occurred at 23:30 on 14 August 2010 was an outlier, the cause was not clear. During the CO<sub>2</sub> release (see Table 1 for the release period), there was no rainfall and the weather was dry. The soil VWC was low (< 0.2 m<sup>3</sup>/m<sup>3</sup>). After the gas was cut off at noon on 15 August, there were a few large precipitation events. Figure 11 shows the comparison of the present model prediction and field observation for the 2010 release experiment. For the 2010 experiment, the VWC was relatively low during the release, and then it greatly increased postrelease. The overall change in the EC is much smaller in the 2010 data than the other years, only approximately 0.17 dS/m from the minimum to the maximum. Similar to Figure 9, the newly calibrated  $pKc$  value is 1.0 for during and after the CO<sub>2</sub> release. The rms error between the model prediction and field observation is 0.0115 dS/m. In the 2010 data set, we can see that the model can predict the bulk soil EC response to dry soil conditions with high soil CO<sub>2</sub> concentration and wet soil conditions where there is little soil CO<sub>2</sub> concentration but a relatively high VWC. The predicted soil EC using Archie's law is also shown in Figure 11. Similar to Figure 9, the newly calibrated  $\sigma_f$  is 2.1. Compared with the measurements, Archie's law can also predict soil EC well, but compared with the present model, the rms error from Archie's law is higher (0.0125 dS/m versus 0.0115 dS/m).

## CASE STUDY TWO: CO<sub>2</sub>-VADOSE PROJECT

### Site description

The second field data set is from the CO<sub>2</sub>-Vadose Project near Girond, France (Le Roux et al., 2013). Experiments on CO<sub>2</sub> release and detection were carried out in 2011 and 2012 (Loisy et al., 2013). Carbon dioxide was released into a controlled environment, and measurements of CO<sub>2</sub> concentration and rock EC were made over several months. The research site for the CO<sub>2</sub>-Vadose Project is in an underground limestone quarry in a carbonate vadose zone at a depth of approximately 7 m. The porosity of the CaCO<sub>3</sub> rock varies

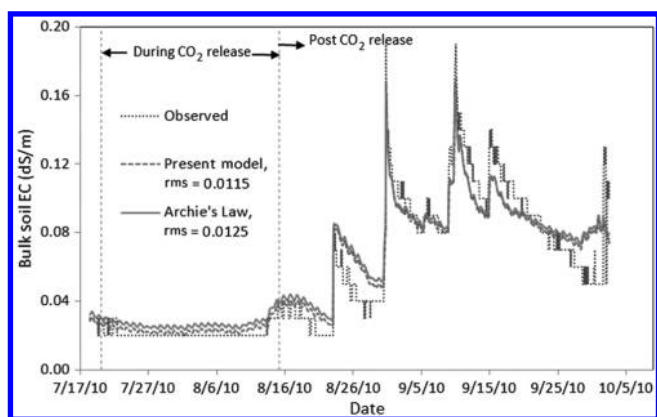


Figure 11. The bulk soil EC data from the 2010 release experiment and model prediction. The vertical dashed lines bracket the time period of CO<sub>2</sub> release. There was very little precipitation during the release time period, but several rain showers afterward; this is visible in the flat EC during the release and increase afterward. Both models can predict the general trends of the observed time series of the soil EC with rms error = 0.0115 dS/m for the present model and with rms error = 0.0125 dS/m for Archie's law.

between 28.5% and 41.5%. The rock temperature is assumed constant at 13°C, and the VWC is assumed constant at the individual array's locations for the duration of the experiment. A comprehensive site description can be found in Loisy et al. (2013). The ERT surveys were conducted by Le Roux et al. (2013) from the surface above the injection room, the top floor and quarry walls of the injection room using direct ER arrays. The data sets collected at the CO<sub>2</sub>-Vadose Project site and used for this study include LB, LMB, and LMH data sets (LB, LMB, and LMH denote three different vertical locations of sensors in the lateral pillar wall of the injection room; see Le Roux et al., 2013). Half of the data set for each location is used for calibration, and the other half is used for evaluation for model prediction.

### Model calibration

Because each data set from the CO<sub>2</sub>-Vadose Project was in a different location and had different physical characteristics, using one set to calibrate the others is not a viable option as with the ZERT data sets, which were collected in different years but at almost the same location. The locations where the various data sets were collected have different porosities; therefore, all the data sets have to be calibrated separately because their cementation exponents may be different. Following the same calibration procedure as the ZERT site, Table 2 shows the results of the calibration and the number of data samples used for calibration. The calibrated values for the chemistry coefficient  $pKc$  at the three locations (LB, LMB, and LMH) are 5.65, 4.80, and 4.95, respectively. The cementation exponents of all the data sets range between 2.5 and 4.2, which are within the range of values found in the literature (see section "Case study one: ZERT site"). The saturation exponent of the LMH data set,  $n = 3.6$ , is a reasonable result. However, the saturation exponents for the LB ( $n = 7.15$ ) and LMB ( $n = 9.85$ ) data sets are larger than those recorded in the literature.

### Model validation

Once the model calibration coefficients have been determined for each data set, they can be applied to the second half of the data sets for validation (Figure 12). The results show that the rms error between the model prediction and observation is less than 0.0004 dS/m for all the data sets.

## DISCUSSION

The analytical model developed in this study can predict the observed soil or rock EC within an rms error of 0.05 or less once it is

Table 2. Summary of the CO<sub>2</sub>-Vadose Project calibration data.

	LB	LMB	LMH
$m$	4.05	4.2	2.5
$n$	7.15	9.85	3.6
$pKc$	5.65	4.80	4.95
rms error	0.0002	0.0003	0.0002
Samples ( $N$ )	123	67	121

calibrated. When looking at the response for a whole season's release, the model does predict the EC well, but there are some indications that under certain conditions, the model will not produce results that are as accurate. The modeled results fit relatively well with the soil EC collected in the field, and the inverted cementation constants are within the range published in the literature. Together, they show that the model represents an estimation of the physical reality but could tolerate refinement, especially at the small magnitudes present in the CO<sub>2</sub>-Vadose Project data sets.

It appears that there needs to be a certain minimum quantity of water in the soil for the CO<sub>2</sub> impact on soil EC to be discernible. This is particularly noticeable in the 2010 ZERT data, in which the soil is quite dry for most of the duration of the release, causing almost no response of the soil EC to changes in soil CO<sub>2</sub> concentration during the release (Figures 9 and 10). It is also apparent during the shutoff (15 August, 18:00) of the 2011 CO<sub>2</sub> release experiment. From the start of the observation, there is a steady drop in the VWC, from approximately 0.27 to 0.17 m<sup>3</sup>/m<sup>3</sup>, and this leads to the expected drop in the EC. The exception to this is the jump from 0.34 to 0.49 dS/m in the EC due to the CO<sub>2</sub> release. The expected drop in EC after the termination of the CO<sub>2</sub> release in the recorded data is due to the decrease in the soil CO<sub>2</sub> concentration and the VWC (Figure 6). Impacts on soil EC due to soil CO<sub>2</sub> and soil VWC are naturally entangled, but it still can be well accounted for by Archie's law, along with the model for CO<sub>2</sub> dissolution and dissociation. Causes for the requirement of a certain level of soil VWC, so that the soil EC responds well to soil CO<sub>2</sub> change, may be multifold: First, as the soil dries out, the water ceases to fill the pores continuously and instead clings to the grains, restricting or even cutting off the pathways for current flow (Corwin and Lesch, 2005). Second, CO<sub>2</sub> dissolution in the water film on the soil particle surface may be saturated quickly, resulting in no further change in soil EC even as the soil CO<sub>2</sub> concentration increases. Third, the contact between the soil matrix and the metal tip of the EC sensor may be compromised as the VWC is reduced to a certain level.

Figures 9 and 11 show that the soil EC changes concurrently with changes in VWC, and VWC is driving most of the variation in EC. However, this does not mean that the influence of the injection of CO<sub>2</sub> is small, because during the release, CO<sub>2</sub> was released at a constant rate, and VWC was the only parameter that varied. The variation of EC due to CO<sub>2</sub> can only be seen by comparing during and after (or before) CO<sub>2</sub> release. A previous analysis of the same data shown in Figure 9 showed that at the same level of soil moisture, the difference in EC between CO<sub>2</sub> release and no-release can be double the value of no-release EC, and this difference increases with increasing soil moisture (Figure 5, Zhou et al., 2012). Figure 2 of this study demonstrates clearly that the soil EC increases with increasing the soil CO<sub>2</sub> concentration, and when the soil moisture is greater, it increases even more rapidly with the soil CO<sub>2</sub> concentration. It may be true that the possible change in water chemistry due to change in various ion concentrations may not be related to the CO<sub>2</sub> injection itself. However, at a CO<sub>2</sub> storage site, a sudden change in water chemistry (and thus the soil EC) should be a serious warning sign that this change may quite possibly be due to the changes in bicarbonate and carbonate concentrations caused by CO<sub>2</sub> leakage.

Temperature dependence of the soil bulk EC was considered in dissolution (equation 3), dissociation (equations 5 and 6), and ionic mobility calculations (equations 10–12). However, results show that

the impact due to VWC and CO<sub>2</sub> concentration during CO<sub>2</sub> release was dominant over that due to the soil temperature. This conclusion was also supported by observation (Zhou et al., 2012). However, we did not observe a change as high as 1%–3% in EC per degree Celsius (Robinson and Stokes, 1965; McCleskey et al., 2012). This probably is related to the amount and type of salt/minerals within the solution.

The quality of the model results can also be tested by the values of calibration constants. As noted in section "Case study one: ZERT site," there is a range for these values that has been published in the literature. The calibration process should produce results that lie within or near to that range. The calibration constant values determined for the ZERT site and LB location at the CO<sub>2</sub>-Vadose Project site fall within the usual range. The calibrated saturation exponents for LB ( $n = 7.15$ ) and LMB ( $n = 9.85$ ) locations at the CO<sub>2</sub>-Vadose Project site are larger than those recorded in the literature.

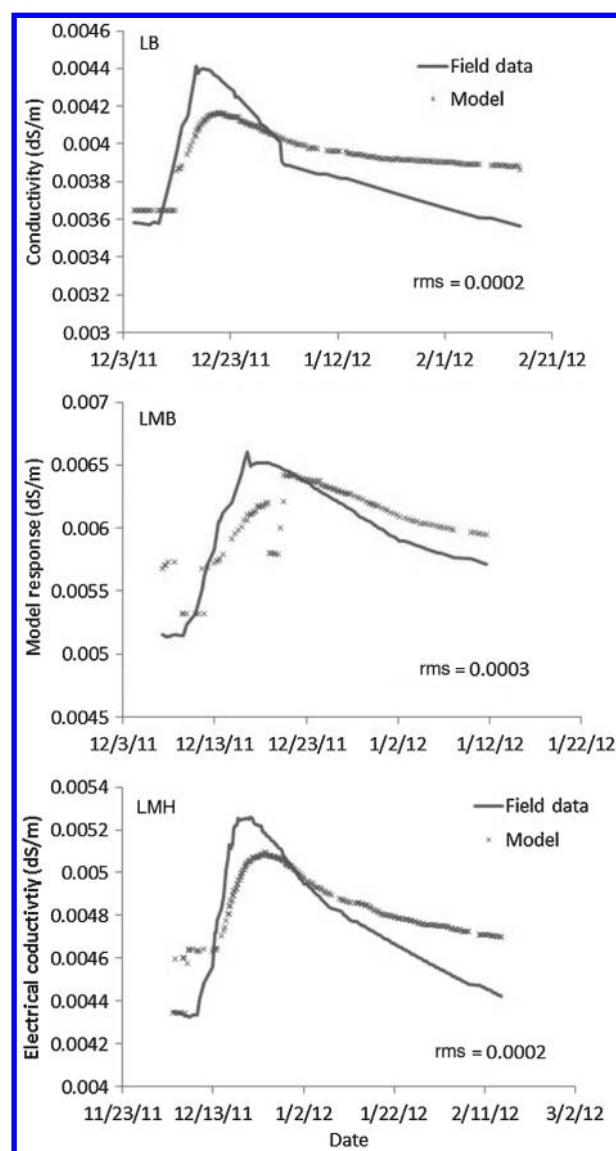


Figure 12. The bulk rock EC data from the CO<sub>2</sub> release experiment and model prediction at three locations at the CO<sub>2</sub>-Vadose Project site.

Given the ambiguous nature of the exponent of saturation and taking it as a tuning parameter, the value at each location combines the effects that are not considered in the model, such as the dynamic effect and surface charges of soil/rock particles, etc., into a single value. Because the number of data samples at LB and LMB locations of the CO<sub>2</sub>-Vadose Project site are relatively small ( $N = 67$  and 121, respectively) compared with those ( $N = 3441$  for 2009, 3654 for 2010, and 22,409 for 2011) at the ZERT site, the representativeness of the calibrated value for the locations at the CO<sub>2</sub>-Vadose Project site might be compromised.

Because values of some model constants, such as  $m$ ,  $n$ ,  $pKc$ , etc., are not usually available or not easily measured, calibration is a way to determine the values of these constants when they are treated as tuning parameters to force the model output to match measured ones from some measurement data sets. Once calibrated, the model output (soil EC) is absolute value. The model can be then be applied to other data sets for validation and ultimately for prediction. The three parameters  $n$ ,  $m$ , and  $pKc$  are usually site dependent and not available, and it is necessary to calibrate the model at each monitoring site. However, model calibration can be done using EC measurement along with VWC, soil temperature, and soil CO<sub>2</sub> measurement without necessarily controlled CO<sub>2</sub> release because CO<sub>2</sub> always exists in soil due to biological processes of soil biota respiration and the decomposition of organic matter. All effects due to numerous ions species (other than those associated with CO<sub>2</sub>) in a real site are lumped into a single parameter; i.e., the chemical constant  $pKc$  (Figure 5), can simplify the problem and make it more practical because no accompanying geochemical measurements to the continuous soil EC monitoring and continuous geochemical monitoring are needed once the parameter is calibrated. However, a functional form can be developed if all ion species can be identified at a real site and the buffering effects and the dissolution and/or precipitation of all ion species (e.g., minerals dissolution) from the soil matrix can be quantified. This could be an interesting endeavor in the future.

## CONCLUSIONS

The CO<sub>2</sub> leakage can be monitored using different methods and strategies. For instance, leaking CO<sub>2</sub> gas can be monitored at the surface using point-based CO<sub>2</sub> gas flux sampling or fluid sampling. However, in comparison with these strategies, the advantages of monitoring EC to infer soil CO<sub>2</sub> for CO<sub>2</sub> leakage detection are multifold: (1) the soil EC monitoring can be continuous in time with high temporal resolution using inexpensive EC or ER probes, (2) continuous EC or ER image of the subsurface can be inferred from EC or ERT methods at surface, and (3) understanding of soil/rock electric properties above CO<sub>2</sub> storage sites in response to leaking CO<sub>2</sub> will help in the development of new techniques in CO<sub>2</sub> storage site monitoring, for instance, electromagnetism-based remote sensing techniques, such as radar.

In summary, an analytical model has been developed for forecasting the bulk soil/rock EC based on the equilibrium chemical and physical processes (dissolution, dissociation, electrolytic conductivity, ion mobility, impact of porosity, and saturation on soil/rock matrix conductivity) of carbonic acid interaction with the soil/rock matrix. But sensitivity study showed the model works best when the VWC exceeds 0.2 m<sup>3</sup>/m<sup>3</sup>. Once the VWC drops below this threshold, the system becomes dominated by the water content of the soil and becomes insensitive to CO<sub>2</sub> impact. Model tests at two com-

pletely different geologic sites showed that the model can predict the trend well of soil/rock EC once it is calibrated. The calibrated values of cementation and saturation coefficients ( $m$  and  $n$ ) are similar to those found within the literature. The model to simulate the soil EC from the ZERT and CO<sub>2</sub>-Vadose Projects was successful in generating a response similar to that observed in the field. At ZERT, the model fitted the observed data with rms error of 0.0115–0.0724 dS/m. For the CO<sub>2</sub>-Vadose Project data, the rms errors were 0.0002–0.0003 dS/m.

## ACKNOWLEDGMENTS

This work was funded by the United States Department of Energy (DOE) Experimental Program to Stimulate Competitive Research program under grant no. DE-FG02-08ER46527 and the ZERT program (DOE award no. DE-FC26-04NT42262). Thanks go to H. Bertete-Aguirre for reviewing the paper and O. Le Roux and the rest of those who worked on the CO<sub>2</sub>-Vadose Project for generously sharing their data. We thank all the reviewers for their very helpful comments and suggestions.

## REFERENCES

- Al Hagrey, S. A., 2011, CO<sub>2</sub> plume modeling in deep saline reservoirs by 2D ERT in boreholes: The Leading Edge, **1**, 25–33, doi: [10.1190/1.3535429](https://doi.org/10.1190/1.3535429).
- Andersen, C. B., 2002, Understanding carbonate equilibria by measuring alkalinity in experimental and natural systems: Journal of Geoscience Education, **50**, 389–403.
- Arts, R. J., B. L. Girard, J. F. Kirby, S. Lombardi, P. Williamson, and A. Zaja, 2009, Results of geophysical monitoring over a “leaking” natural analogue site in Italy: Energy Procedia, **1**, 2269–2276, doi: [10.1016/j.egypro.2009.01.295](https://doi.org/10.1016/j.egypro.2009.01.295).
- Banisi, S., J. A. Finch, and A. R. Laplante, 1993, Electrical conductivity of dispersions: A review: Minerals Engineering, **6**, 369–385, doi: [10.1016/0892-6875\(93\)90016-G](https://doi.org/10.1016/0892-6875(93)90016-G).
- Barta, L., 1982, Extension of the ion interaction model for brines to include gas solubilities and the volumetric properties of weak electrolytes: M.S. thesis, Montana College of Mineral Science and Technology.
- Berg, C. F., 2012, Re-examining Archie’s law: Conductance description by tortuosity and constriction: Physical Review E, **86**, 046314, doi: [10.1103/PhysRevE.86.046314](https://doi.org/10.1103/PhysRevE.86.046314).
- Bigalke, J., 2000, A study concerning the conductivity of porous rock: Physical Chemistry of the Earth (A), **25**, 189–194, doi: [10.1016/S1464-1895\(00\)00030-2](https://doi.org/10.1016/S1464-1895(00)00030-2).
- Breen, S. J., C. R. Carrigan, D. J. LaBrecque, and R. L. Detwiler, 2012, Bench-scale experiments to evaluate electrical resistivity tomography as a monitoring tool for geologic CO<sub>2</sub> sequestration: International Journal of Greenhouse Gas Control, **9**, 484–494, doi: [10.1016/j.ijggc.2012.04.009](https://doi.org/10.1016/j.ijggc.2012.04.009).
- Bristow, L. B., G. J. Kluitenberg, C. J. Goding, and T. S. Fitzgerald, 2001, A small multi-needle probe for measuring soil thermal properties, water content and electrical conductivity: Computers and Electronics in Agriculture, **31**, 265–280, doi: [10.1016/S0168-1699\(00\)00186-1](https://doi.org/10.1016/S0168-1699(00)00186-1).
- Carrigan, C. R., X. Yang, D. J. LaBrecque, D. Larsen, D. Freeman, A. L. Ramirez, W. Daily, R. Aines, R. Newmark, J. Friedmann, and S. Hovorka, 2013, Electrical resistance tomographic monitoring of CO<sub>2</sub> movement in deep geologic reservoirs: International Journal of Greenhouse Gas Control, **18**, 401–408, doi: [10.1016/j.ijggc.2013.04.016](https://doi.org/10.1016/j.ijggc.2013.04.016).
- Carroll, J. J., J. D. Slupsky, and A. E. Mather, 1991, The solubility of carbon dioxide in water at low pressure: Journal of Physical and Chemistry Reference Data, **20**, 1201–1209, doi: [10.1063/1.555900](https://doi.org/10.1063/1.555900).
- Corwin, D. L., and S. M. Lesch, 2005, Apparent soil electrical conductivity measurements in agriculture: Computers and Electronics in Agriculture, **46**, 11–43, doi: [10.1016/j.compag.2004.10.005](https://doi.org/10.1016/j.compag.2004.10.005).
- Coury, L., 1999, Conductance measurements. Part 1: Theory: Current Separations, **18**, 91–96.
- Dafflon, B., Y. Wu, S. S. Hubbard, J. T. Birkholzer, T. M. Daley, J. D. Pugh, J. E. Peterson, and R. C. Trautz, 2013, Monitoring CO<sub>2</sub> intrusion and associated geochemical transformations in a shallow groundwater system using complex electrical methods: Environmental Science and Technology, **47**, 314–321, doi: [10.1021/es301260e](https://doi.org/10.1021/es301260e).
- Dickinson, E. J. F., J. G. Limon-Petersen, and R. G. Compton, 2011, The electroneutrality approximation in electrochemistry: Journal of Solid State Electrochemistry, **15**, 1335–1345, doi: [10.1007/s10008-011-1323-x](https://doi.org/10.1007/s10008-011-1323-x).

- England, A. H., A. M. Duffin, C. P. Schwartz, J. S. Uejio, D. Prendergast, and R. J. Saykally, 2011, On the hydration and hydrolysis of carbon dioxide: *Chemical Physics Letters*, **514**, 187–195, doi: [10.1016/j.cplett.2011.08.063](https://doi.org/10.1016/j.cplett.2011.08.063).
- Enick, R. M., and S. M. Klara, 1990, CO<sub>2</sub> solubility in water and brine under reservoir conditions: *Chemical Engineering Communications*, **90**, 23–33, doi: [10.1080/00986449008940574](https://doi.org/10.1080/00986449008940574).
- Fabriol, H., A. Bitri, B. Bourgeois, M. Delatre, J. F. Girard, G. Pajot, and J. Rohmer, 2011, Geophysical methods for CO<sub>2</sub> plume imaging: Comparison of performances: *Energy Procedia*, **4**, 3604–3611, doi: [10.1016/j.egypro.2011.02.290](https://doi.org/10.1016/j.egypro.2011.02.290).
- Friedman, S. P., 2005, Soil properties influencing apparent electrical conductivity: A review: *Computers and Electronics in Agriculture*, **46**, 45–70, doi: [10.1016/j.compag.2004.11.001](https://doi.org/10.1016/j.compag.2004.11.001).
- Gasperikova, E., and G. M. Hovsten, 2006, A feasibility study of nonseismic geophysical methods for monitoring geologic CO<sub>2</sub> sequestration: *The Leading Edge*, **10**, 1282–1288, doi: [10.1190/l.2360621](https://doi.org/10.1190/l.2360621).
- Georgaki, I., P. Soupios, N. Sakkas, F. Ververidis, E. Trantas, F. Vallianatos, and T. Manios, 2008, Evaluating the use of electrical resistivity imaging technique for improving CH<sub>4</sub> and CO<sub>2</sub> emission rate estimations in landfills: *Science of the Total Environment*, **389**, 522–531, doi: [10.1016/j.scitotenv.2007.08.033](https://doi.org/10.1016/j.scitotenv.2007.08.033).
- Glover, P., 2009, What is the cementation exponent? A new interpretation: *The Leading Edge*, **1**, 82–85, doi: [10.1190/l.3064150](https://doi.org/10.1190/l.3064150).
- Gomaa, E. A., and B. M. Al-Jahdali, 2012, Conductometric studies of ionic association of divalent asymmetric electrolyte Cu(NO<sub>3</sub>)<sub>2</sub> with Kryptofix-22 in mixed (MeOH-DMF) solvents at different temperatures: *American Journal of Condensed Matter Physics*, **2**, 16–21, doi: [10.5923/j.ajcmp.20120201.03](https://doi.org/10.5923/j.ajcmp.20120201.03).
- Grellier, S., H. Robain, G. Bellier, and N. Skhiri, 2006, Influence of temperature on the electrical conductivity of leachate from municipal solid waste: *Journal of Hazardous Materials*, **B137**, 612–617, doi: [10.1016/j.jhazmat.2006.02.049](https://doi.org/10.1016/j.jhazmat.2006.02.049).
- Holloway, S., 2001, Storage of fossil fuel-derived carbon dioxide beneath the surface of the earth: *Annual Review of Energy and the Environment*, **26**, 145–166, doi: [10.1146/annurev.energy.26.1.145](https://doi.org/10.1146/annurev.energy.26.1.145).
- Hovorka, S. D., T. A. Meckel, R. H. Trevino, J. Lu, J. Nicot, J. Choi, D. Freeman, P. Cook, T. M. Daley, J. B. Ajo-Franklin, B. M. Freifeild, C. Doughty, C. R. Carrigan, D. La Brecque, Y. K. Kharaka, J. J. Thordsen, T. J. Phelps, C. Yang, K. D. Romanak, T. Zhang, R. M. Holt, J. S. Lindler, and R. J. Butsch, 2011, Monitoring a larger volume CO<sub>2</sub> injection: Year two results from SECARB project at Denbury's Cranfield, Mississippi, USA: *Energy Procedia*, **4**, 3478–3485, doi: [10.1016/j.egypro.2011.02.274](https://doi.org/10.1016/j.egypro.2011.02.274).
- Kestin, J., M. Sokolov, and W. A. Wakeham, 1978, Viscosity of liquid water in the range –8°C to 150°C: *Journal of Chemical Reference Data*, **7**, 941–948, doi: [10.1063/1.555581](https://doi.org/10.1063/1.555581).
- Kharaka, Y. K., J. J. Thordsen, E. Kakouros, G. Ambats, W. N. Herkelrath, S. R. Beers, J. T. Birkholzer, J. A. Apps, N. F. Spycher, L. Zheng, R. C. Trautz, H. W. Rauch, and K. S. Gullickson, 2010, Changes in the chemistry of shallow groundwater related to the 2008 injection of CO<sub>2</sub> at the ZERT field site, Bozeman, Montana: *Environmental Earth Science*, **60**, 273–284, doi: [10.1007/s12665-009-0401-1](https://doi.org/10.1007/s12665-009-0401-1).
- Kiessling, D., C. Schmidt-Hattenberger, H. Schuett, F. Schilling, K. Krueger, B. Schoebel, E. Danckardt, and J. Kummerow, 2010, Geoelectrical methods for monitoring geological CO<sub>2</sub> storage: First results from the cross-hole and surface-downhole measurements from the CO<sub>2</sub>SINK test site at Ketzin (Germany): *International Journal of Greenhouse Gas Control*, **4**, 816–826, doi: [10.1016/j.ijggc.2010.05.001](https://doi.org/10.1016/j.ijggc.2010.05.001).
- Lakkaraju, V. R., X. Zhou, M. Apple, A. Cunningham, L. M. Dobeck, K. Gullickson, and L. H. Spangler, 2010, Studying the vegetation response to the simulated leakage of sequestered CO<sub>2</sub> using spectral vegetation indices: *Ecological Informatics*, **5**, 379–389, doi: [10.1016/j.ecoinf.2010.05.002](https://doi.org/10.1016/j.ecoinf.2010.05.002).
- Laloy, E., M. Javaux, M. Vanclooster, C. Roisin, and C. L. Bielders, 2011, Electrical resistivity in a loamy soil: Identification of the appropriate pedo-electrical model: *Vadose Zone Journal*, **10**, 1023–1033.
- Langmuir, D., 1997, *Aqueous environmental geochemistry*: Simon & Schuster.
- Le Roux, O., G. Cohen, C. Loisy, C. Laveuf, P. Delaplace, C. Magnier, V. Rouchon, A. Cerepi, and B. Garcia, 2013, The CO<sub>2</sub>-Vadose Project: Time-lapse geoelectrical monitoring during CO<sub>2</sub> diffusion in the carbonate vadose zone: *International Journal of Greenhouse Gas Control*, **16**, 156–166, doi: [10.1016/j.ijggc.2013.03.016](https://doi.org/10.1016/j.ijggc.2013.03.016).
- Li, Z., M. Dong, S. Li, and S. Huang, 2006, CO<sub>2</sub> sequestration in depleted oil and gas reservoirs — Caprock characterization and storage capacity: *Energy Conversion and Management*, **47**, 1372–1382, doi: [10.1016/j.enconman.2005.08.023](https://doi.org/10.1016/j.enconman.2005.08.023).
- Liu, F., P. Lu, C. Griffith, S. W. Hedges, Y. Soong, H. Hellevang, and C. Zhu, 2012, CO<sub>2</sub>-brine-caprock interaction: Reactivity experiments on Eau Claire shale and a review of relevant literature: *International Journal of Greenhouse Gas Control*, **7**, 153–167, doi: [10.1016/j.ijggc.2012.01.012](https://doi.org/10.1016/j.ijggc.2012.01.012).
- Loisy, C., G. Cohen, C. Laveuf, O. Le Roux, P. Delaplace, C. Magnier, V. Rouchon, A. Cerepi, and B. Garcia, 2013, The CO<sub>2</sub>-Vadose Project: Dynamics of the natural CO<sub>2</sub> in a carbonate vadose zone: *International Journal of Greenhouse Gas Control*, **14**, 97–112, doi: [10.1016/j.ijggc.2012.12.017](https://doi.org/10.1016/j.ijggc.2012.12.017).
- Longinelli, A., L. Langone, C. Ori, F. Giglio, E. Selmo, and M. Sgavetti, 2013, Atmospheric CO<sub>2</sub> concentrations and δ<sup>13</sup>C values during 2011–2012 voyage: Mediterranean, Atlantic Ocean, southern Indian Ocean and New Zealand to Antarctica: *Atmospheric Environment*, **77**, 919–926.
- McCleskey, R. B., D. K. Nordstrom, J. N. Ryan, and J. W. Ball, 2012, A new method of calculating electrical conductivity with applications to natural waters: *Geochimica et Cosmochimica Acta*, **77**, 369–382, doi: [10.1016/j.gca.2011.10.031](https://doi.org/10.1016/j.gca.2011.10.031).
- Mook, W. G., 2000, Environmental isotopes in the hydrological cycle, principles and applications. vol. 1: Introduction, theory, methods, review: International Atomic Energy Agency and UNESCO.
- Rein, A., R. Hoffmann, and P. Dietrich, 2004, Influence of natural time-dependent variations of electrical conductivity on DC resistivity measurements: *Journal of Hydrology*, **285**, 215–232, doi: [10.1016/j.jhydrol.2003.08.015](https://doi.org/10.1016/j.jhydrol.2003.08.015).
- Rhoades, J. D., and D. L. Corwin, 1990, Soil electrical conductivity: Effects of soil properties and application to soil salinity appraisal: *Communications in Soil Science and Plant Analysis*, **21**, 837–860, doi: [10.1080/00103629009368274](https://doi.org/10.1080/00103629009368274).
- Robinson, R. A., and R. H. Stokes, 1965, *Electrolyte solutions*: Butterworth Publications Limited.
- Samoulian, A., I. Cousin, A. Tabbagh, A. Bruand, and G. Richard, 2005, Electrical resistivity survey in soil science: A review: *Soil & Tillage Research*, **83**, 173–193, doi: [10.1016/j.still.2004.10.004](https://doi.org/10.1016/j.still.2004.10.004).
- Sauck, W. A., 2000, A model for the resistivity structure of LNAPL plumes and their environs in sandy sediments: *Journal of Applied Geophysics*, **44**, 151–165, doi: [10.1016/S0926-9851\(99\)00021-X](https://doi.org/10.1016/S0926-9851(99)00021-X).
- Seger, M., I. Cousin, A. Frison, H. Boizard, and G. Richard, 2009, Characterization of the structural heterogeneity of the soil tilled layer by using in situ 2D and 3D electrical resistivity measurements: *Soil & Tillage Research*, **103**, 387–398, doi: [10.1016/j.still.2008.12.003](https://doi.org/10.1016/j.still.2008.12.003).
- Sharma, B., M. E. Apple, X. Zhou, J. M. Olson, C. Dorshorst, L. M. Dobeck, A. B. Cunningham, and L. Spangler, 2014, Physiological responses of Dandelion and Orchard grass leaves to experimentally released upwelling soil CO<sub>2</sub>: *International Journal of Greenhouse Gas Control*, **24**, 139–148, doi: [10.1016/j.ijggc.2014.03.006](https://doi.org/10.1016/j.ijggc.2014.03.006).
- Shukla, R., P. Ranjith, A. Haque, and X. Choi, 2010, A review of studies on CO<sub>2</sub> sequestration and caprock integrity: *Fuel*, **89**, 2651–2664, doi: [10.1016/j.fuel.2010.05.012](https://doi.org/10.1016/j.fuel.2010.05.012).
- Singha, K., L. Li, F. D. Day-Lewis, and A. B. Regberg, 2011, Quantifying solute transport processes: Are chemically “conservative” tracers electrically conservative?: *Geophysics*, **76**, no. 1, F53–F63, doi: [10.1190/1.3511356](https://doi.org/10.1190/1.3511356).
- Spangler, L. H., L. M. Dobeck, K. S. Repasky, A. R. Nehr, S. D. Humphries, J. L. Barr, C. J. Keith, J. A. Shaw, J. H. Rouse, A. B. Cunningham, S. M. Benson, C. M. Oldenburg, J. L. Lewicki, A. W. Wells, J. R. Diehl, B. R. Strazisar, J. E. Fessenden, T. A. Rahn, J. E. Amonette, J. L. Barr, W. L. Pickles, J. D. Jacobson, E. A. Silver, E. J. Male, H. W. Rauch, K. S. Gullickson, R. Trautz, Y. Kharaka, J. Birkholzer, and L. Wielopolski, 2009, A shallow subsurface controlled release facility in Bozeman, Montana, USA, for testing near surface CO<sub>2</sub> detection techniques and transport models: *Environmental Earth Sciences*, **60**, 227–239, doi: [10.1007/s12665-009-0400-2](https://doi.org/10.1007/s12665-009-0400-2).
- Strazisar, B. R., A. W. Wells, J. R. Diehl, R. W. Hammack, and G. A. Veloski, 2009, Near-surface monitoring for the ZERT shallow CO<sub>2</sub> injection project: *International Journal of Greenhouse Gas Control*, **3**, 736–744, doi: [10.1016/j.ijggc.2009.07.005](https://doi.org/10.1016/j.ijggc.2009.07.005).
- Thomson, A. M., G. P. Kyle, X. Zhang, V. Bandaru, T. O. West, M. A. Wise, R. C. Izaurralde, and K. V. Calvin, 2014, The contribution of future agricultural trends in the US Midwest to global climate change mitigation: *Global Environmental Change*, **24**, 143–154, doi: [10.1016/j.gloenvcha.2013.11.019](https://doi.org/10.1016/j.gloenvcha.2013.11.019).
- Visconti, F., J. M. de Paz, and J. L. Rubio, 2010, An empirical equation to calculate soil solution electrical conductivity at 25°C from major ion concentrations: *European Journal of Soil Science*, **61**, 980–993, doi: [10.1111/j.1365-2389.2010.01284.x](https://doi.org/10.1111/j.1365-2389.2010.01284.x).
- Wang, P., A. Anderko, and R. D. Young, 2004, Modeling electrical conductivity in concentrated and mixed-solvent electrolyte solutions: *Industrial & Engineering Chemistry Research*, **43**, 8083–8092, doi: [10.1021/ie040144c](https://doi.org/10.1021/ie040144c).
- Xiao, Y., T. Xu, and K. Pruess, 2009, The effects of gas-fluid-rock interaction on CO<sub>2</sub> injection and storage: Insights from reactive transport modeling: *Energy Procedia*, **1**, 1783–1790, doi: [10.1016/j.egypro.2009.01.233](https://doi.org/10.1016/j.egypro.2009.01.233).
- Yan, W., S. Huang, and E. H. Stenby, 2011, Measurement and modeling of CO<sub>2</sub> solubility in NaCl brine and CO<sub>2</sub>-saturated NaCl brine density:

- International Journal of Greenhouse Gas Control, **5**, 1460–1477, doi: [10.1016/j.ijggc.2011.08.004](https://doi.org/10.1016/j.ijggc.2011.08.004).
- Zhang, Y., C. Oldenburg, S. Finsterle, P. Jordan, and K. Zhang, 2009, Probability estimation of CO<sub>2</sub> leakage through faults at geologic carbon sequestration sites: *Energy Procedia*, **1**, 41–46, doi: [10.1016/j.egypro.2009.01.008](https://doi.org/10.1016/j.egypro.2009.01.008).
- Zhou, X., M. Apple, L. M. Dobeck, A. B. Cunningham, and L. H. Spangler, 2013, Observed response of soil O<sub>2</sub> concentration to leaked CO<sub>2</sub> from an engineered CO<sub>2</sub> leakage experiment: *International Journal of Greenhouse Gas Control*, **16**, 116–128, doi: [10.1016/j.ijggc.2013.03.005](https://doi.org/10.1016/j.ijggc.2013.03.005).
- Zhou, X., V. Lakkaraju, M. Apple, L. M. Dobeck, K. Gullickson, J. A. Shaw, A. B. Cunningham, L. Wielopolski, and L. H. Spangler, 2012, Experimental observation of signature changes in bulk soil electrical conductivity in response to engineered surface CO<sub>2</sub> leakage: *International Journal of Greenhouse Gas Control*, **7**, 20–29, doi: [10.1016/j.ijggc.2011.12.006](https://doi.org/10.1016/j.ijggc.2011.12.006).
- Ziabakhsh-Ganji, Z., and H. Kooi, 2012, An equation of state for thermodynamic equilibrium of gas mixtures and brines to allow simulation of the effects of impurities in subsurface CO<sub>2</sub> storage: *International Journal of Greenhouse Gas Control*, **11S**, S21–S34, doi: [10.1016/j.ijggc.2012.07.025](https://doi.org/10.1016/j.ijggc.2012.07.025).